ANNALS OF PHYSICS 187, 471–501 (1988)

First-Forbidden Beta Decay near $A = 40$

E. K. WARBURTON

Brookhaven National Laboratory, Upton, New York 11973

J. A. BECKER

Lawrence Livermore Laboratory, Livermore, California 94550

B. A. BROWN

Michigan State University, Cyclotron Laboratory, East Lansing, Michigan 48824

AND

D. J. MILLENER

Brookhaven National Laboratory, Upton, New York 11973

Received June 14, 1988

Shell model calculations in the full *sdpf* model space are carried out for the known and possible first-forbidden beta decays for $34 < A < 44$. The main purpose is to study the strong quenching of the unique ($\Delta J = 2$) decays, which results from the repulsive nature of the $T = 1$ particle–hole interaction, and the strong meson-exchange enhancement of the $\Delta J = 0$ decays. Procedures for calculating the relevant matrix elements and combining them to form the decay rate are described in detail. Various approximations designed to display more clearly the dependence of the rates on the contributing matrix elements are presented and the associated errors assessed. The results are compared to experiment and conclusions are drawn regarding our present understanding of first-forbidden beta decays.

A. INTRODUCTION

The study of first-forbidden beta decay has revealed two unusual and initially startling phenomena which have allowed a better understanding of the basic nature of the interaction of nucleons within the nucleus. The first of these phenomena to be studied was the strong quenching of the unique ($\Delta J = 2$, e.g., $0^+ \leftrightarrow 2^-$) rates [1, 2] which can be traced to the repulsive nature of the $T = 1$ particle–hole interaction. More recently, Kubodera, Delorme, and Rho [3] used chiral-symmetry arguments and soft-pion theorems to predict a very large ($\sim$40–70 %) enhancement over the impulse approximation for the time-like component of the axial current in nuclear

0003-4916/88 $7.50

595/187/2-15

processes. The enhancement, due to meson-exchange contributions to the matrix element of γ_5, is most easily studied via first-forbidden beta decay between states of the same spin—for instance $0^+ \leftrightarrow 0^-$ decays—and such studies near $A = 16$ appear to verify the prediction [4, 5].

The main motive for the present work was to further study these two phenomenon in the $A = 34$–44 region. First-forbidden beta decay ($\Delta J \leqslant 2$, $\pi_i \pi_f = -$) occurs near closed shells where the valence nucleons of initial and final states occupy orbits of opposite parity. The $A = 34$–44 region supplies the bulk of the information used in the pioneer study of unique decays [1, 2]. In that study effects of the full *sdpf* model space were added perturbatively to a $d_{3/2} f_{7/2}$ calculation. In this study we will go a step further by diagonalizing in the full $0\hbar\omega$ and $1\hbar\omega$ *sdpf* model spaces. Extensive calculations of first-forbidden $\Delta J = 0$ transitions have been made by two of us for the nuclei near ^{16}O [5–10]. Prior to the present efforts—some results of which have been previously reported [11]—there have been no calculations of $\Delta J = 0$ or 1 transitions for the $A = 40$ region.

This lack of attention is typical of the general situation. First-forbidden beta decay is an under-utilized tool in nuclear spectroscopy and, more important, is relatively poorly understood. To illustrate this latter point, consider that the effects of the nuclear medium on Fermi and Gamow–Teller decays have been the subject of exhaustive investigation. In particular, detailed experimental and theoretical information is available concerning the quenching of g_A in nuclear matter via core excitations, meson-exchange currents, isobar currents, etc. [12, 13]. By contrast, our understanding of the $\Delta J = 2$ first-forbidden decay rates in the $A = 34$–44 region has not advanced theoretically since 1971 when the matrix elements were calculated in a highly truncated model space; and the $\Delta J < 2$ rates have not been considered at all. The description of these decays is relatively complicated and involves matrix elements which are quite sensitive to details of the interaction and to the single-particle wavefunctions. From general considerations and from experience in the $A = 16$ region, it is clear that quite sophisticated shell-model calculations are necessary in order to assess the information which can be obtained from the $A = 34$–44 region on the effects of nuclear matter on the first-forbidden operators.

With this background in mind, the purpose of the present work is to catalog the known and possible first-forbidden decays in the $A = 34$–44 region, to calculate the theoretical decay rates, and to compare experiment to theory. The principal motive is to provide a better general understanding of first-forbidden decays. A second motive is to search for cases which might, through detailed study, provide information of a fundamental nature on such phenomena as the aforementioned meson-exchange enhancement of $\Delta J = 0$ transitions and the repulsive nature of the $T = 1$ particle–hole interaction. Finally, the theoretical study of first-forbidden decays cannot help but provide valuable spectroscopic information.

There are two alternate formalisms used in the calculation of first-forbidden beta decay: those of Behrens and Buhring [14] and of Walecka [15]. The Behrens–Buhring formalism is exact (in principle) and we shall use it. The Walecka treatment neglects certain terms proportional to the nuclear charge and also the neutron–

proton mass difference. The difference between the two treatments is small for the rather large energy releases encountered in most of the decays of interest here; however, for small $\beta^{\mp}$ Q values—e.g., $^{18}\mathrm{Ne}(\beta^{+})^{18}\mathrm{F}$—the difference can be large.

The calculation of first-forbidden decay rates via the impulse approximation in the nuclear shell model naturally involves three steps: first, the calculation of the one-body density matrix elements (OBDME); second, the calculation from these OBDME of the first-forbidden matrix elements of which there are generally six; third, the combination of the matrix elements to obtain a decay rate. The calculation of the OBDMEs is a straightforward application of a shell-model code. We use OXBASH [16]. The first-forbidden decays under consideration involve nucleon transitions between the ($2s$, $1d$) and ($1f$, $2p$) major shells. We shall describe these transitions via a cross-shell interaction involving the full ($2s$, $1d$)($1f$, $2p$) configurational space. This *sdpf* interaction—designated WBMB—has been fully described previously [17]; it is similar to one used in recent calculations of some unique first-forbidden decays [18]. The first-forbidden matrix elements are defined in Section B. In Section C we discuss the effect on these matrix elements of shortcomings of the impulse approximation (nucleons in a nucleus do not act as if they were in free space) and truncation to the WBMB model space. The calculation of the decay rate is taken up in Section D and some useful definitions and approximations are presented in Section E. The notation used in first-forbidden beta decay has developed historically and has not been unified. In the present treatment we shall attempt to display as clearly as possible the relationships between our formalism and previous or alternative ones. In Sections F and G we describe the shell-model calculations and compare them to experiment. Section H contains predictions for unobserved transitions. The findings are summarized in Section I.

B. Definition of the Matrix Elements

Nuclear matrix elements of the following two classes of one-body operators,

$$\underline{r},\ [\underline{r},\ \underline{\sigma}\,]^{R},\ \text{where } R = 0,\ 1,\ 2, \tag{1}$$

and

$$\gamma_5,\ \underline{\alpha},$$

are required in an analysis of first-forbidden beta decay in the impulse approximation. The nonrelativistic operators of the first group come from an expansion of the lepton wavefunctions, while those in the second group occur in the hadronic weak current. They connect the large and small components of nucleonic wavefunctions and are referred to as relativistic. In Eq. (1), R represents the rank of the operator. Matrix elements of different rank add incoherently in forming the

decay rate. Also, the contribution to a given decay between states of J_i and J_f has the selection rule

$$|J_i - J_f| \leqslant R \leqslant J_i + J_f. \tag{2}$$

Thus the rank R is a very useful concept in understanding and classifying first-forbidden decays. In Eq. (1) the operator $\underline{r}$ is the analog of the E1 operator and has rank 1 (R1) while γ_5 and $\underline{\alpha}$ are R0 and R1, respectively. The desired matrix elements and the symbols used to represent them are [6, 19, 20]

$$M_0^S = \lambda \sqrt{3}\, \langle J_f T_f \| ir[C_1, \boldsymbol{\sigma}]^0 \boldsymbol{\tau} \| J_i T_i \rangle C,$$

where $C_L = [4\pi/(2L+1)]^{1/2} Y_L$,

$$\begin{aligned} x &= -\langle J_f T_f \| irC_1 \boldsymbol{\tau} \| J_i T_i \rangle C, \\ u &= \lambda \sqrt{2}\, \langle J_f T_f \| ir[C_1, \boldsymbol{\sigma}]^1 \boldsymbol{\tau} \| J_i T_i \rangle C, \\ z &= -\lambda 2 \langle J_f T_f \| ir[C_1, \boldsymbol{\sigma}]^2 \boldsymbol{\tau} \| J_i T_i \rangle C, \end{aligned} \tag{3}$$

where $\lambda = -C_A/C_V = 1.2605$ is taken from an analysis of neutron beta decay [21]. In Eq. (3) and throughout Section B, all quantities are in natural units unless otherwise stated;

$$C = \langle T_i M_i 1 \pm 1 \mid T_f M_f \rangle \hat{J}_f / (\sqrt{2}\, \hat{J}_i)$$

for $\beta^{\mp}$ decay, and the matrix elements, reduced in both J and T, are according to the definition of Brink and Satchler [22]. Unless otherwise stated, matrix elements are evaluated with harmonic oscillator wavefunctions calculated with an oscillator length $b = (41.467/\hbar\omega)^{1/2}$ fm with $\hbar\omega = 45A^{-1/3} - 25A^{-2/3}$ MeV.

In the Behrens–Bühring formulation [14] the beta decay formulae are derived by expanding the electron radial wavefunctions in powers of the mass and energy parameters of the electron and of the nuclear charge. In this treatment additional matrix elements occur which contain both the nuclear and the electromagnetic structure of the nucleus via the shape of the nuclear charge distribution. The use of a uniform charge distribution of radius r_u is a very good approximation provided it implies the correct experimental *rms* size of the nucleus We use for r_u the expression given by Brown *et al.* [23]. The extra matrix elements needed are obtained from the definitions of M_0^S, x, and u by including in the radial integral an extra factor [14]

$$\begin{aligned} \frac{2}{3} I(1,1,1,1;r) &= \left[1 - \frac{1}{5}\left(\frac{r}{r_u}\right)^2\right], \qquad 0 < r < r_u \\ &= \left[\frac{R}{r} - \frac{1}{5}\left(\frac{r_u}{r}\right)^3\right], \qquad r > r_u \end{aligned} \tag{4}$$

and are denoted $M_0^{S\prime}$, x', and u'. The ratios of the primed to unprimed quantities are fairly insensitive to details of the nuclear structure and are roughly 0.7. We denote these ratios r'_w, r'_x, r'_u, respectively. We sometimes use a ratio of 0.7 in approximations made to better understand the underlying structure of specific decays. The relativistic matrix elements, of $\gamma_5\tau$ and $\boldsymbol{\alpha}\tau$, are

$$\begin{aligned} M_0^{T} &= \lambda\langle J_f T_f \| \gamma_5 \tau \| J_i T_i \rangle C, \\ \xi' y &= -\langle J_f T_f \| \boldsymbol{\alpha}\tau \| J_i T_i \rangle C. \end{aligned} \tag{5}$$

We have adopted the notation M_0^{S} and M_0^{T} [24] for the two R0 matrix elements of Eqs. (3), (5) because it more readily indicates that they are the space-like and time-like components of the R0 axial current, which are presently of much interest [3, 4]; the notation M_0^{S} and M_0^{T} replaces the w and $\xi' v$ of Schopper [19]. These are all the matrix elements which enter in dominant order, i.e., in leading order in an expansion in terms of the electron mass, m_e, the electron energy W, and the nuclear charge, Z. Higher-order terms are completely negligible in any application we have encountered to date. In evaluating M_0^{T} and $\xi' y$ the usual nonrelativistic replacements for γ_5 and $\boldsymbol{\alpha}$ can be made yielding

$$\begin{aligned} M_0^{T} &= -\lambda\sqrt{3}\left\langle J_f T_f \left\| \frac{i}{M_N}[\boldsymbol{\sigma}, \boldsymbol{\nabla}]^0 \tau \right\| J_i T_i \right\rangle C, \\ \xi' y &= -\left\langle J_f T_f \left\| \frac{i}{M_N}\boldsymbol{\nabla}\tau \right\| J_i T_i \right\rangle C, \end{aligned} \tag{6}$$

where M_N is the mass of the nucleon. These approximations are accurate to order $1/M_N$. The conserved vector current (CVC) theory may be used [14, 25] to obtain an alternative expression for $\xi' y$ in terms of x and a similar nonrelativistic matrix element involving the Coulomb field of the nucleus. Under the strong assumption—which we adopt—that isospin is a good quantum number one has [26]

$$\xi' y = E_\gamma x. \tag{7}$$

In this way the number of independent matrix elements can be reduced by one. Several examples which illustrate the energetics involved in the relationship of Eq. (7) are given in Fig. 1. If we denote an analog of the initial state by $a(i)$ and of the final state by $a(f)$, we have that

$$E_\gamma = E[a(i)] - E[f] \tag{8a}$$

if the gamma transition occurs in the final nucleus or

$$E_\gamma = E[i] - E[a(f)], \tag{8b}$$

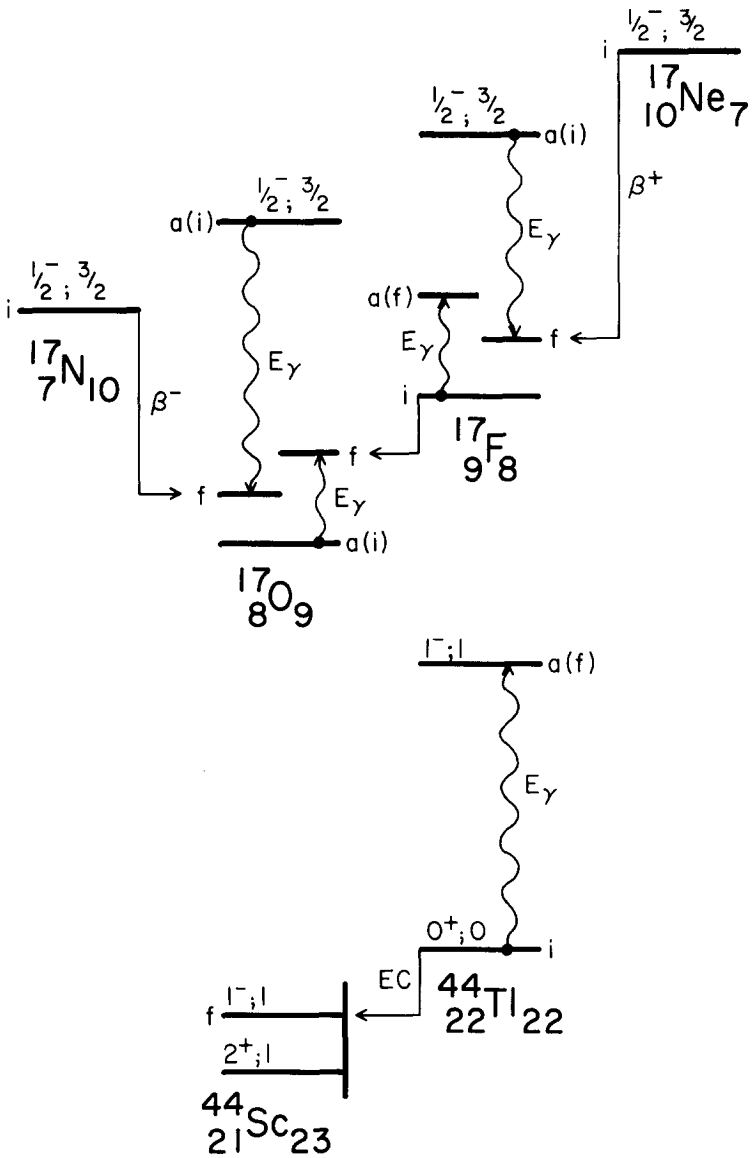

FIG. 1. Examples illustrating the energetics involved in the CVC relationship of Eq. (7). J; T values are given for some levels. Energies are not to scale and the $^{17}F(\beta^+)^{17}O$ decay (to a presumed $\frac{5}{2}^-$; $\frac{1}{2}$ state) is partly hypothetical. E_γ is positive for downgoing and negative for upgoing arrows. Initial states are labeled i and final states f; their analogs are labeled $a(i)$ or $a(f)$.

if it occurs in the initial nucleus. We can use a measured radiative width for the E1 transition to obtain the magnitude of x. Thus,

$$|x| = [(8\pi/3)\, B(\mathrm{E1}; i \to f) \langle T_i M_i 1 \pm 1 \mid T_f M_f \rangle^2 / \langle T_i M 10 \mid T_f M \rangle^2]^{1/2}, \qquad (9)$$

where the ± 1 sign refers to $\beta^{\mp}$ decay and M can be M_i or M_f. In Eq. (9), $B(\mathrm{E1}; i \to f)$ is in units of fm^2 and can be deduced from

$$\Gamma_\gamma(\mathrm{eV}) = 1.04653[E_\gamma\,(\mathrm{MeV})]^3\, B(\mathrm{E1}; i \to f) \qquad (10)$$

if E_γ is positive. If E_γ is negative we need $B(\mathrm{E1}\uparrow)$, and the right-hand side of Eq. (10) must be equated to $[(2J_f+1)/(2J_i+1)]\,\Gamma_\gamma$. In the case of transitions between mirror nuclei, e.g., $^{19}\mathrm{Ne}(\frac{1}{2}^+; gs) \to {}^{19}\mathrm{F}(\frac{1}{2}^-;\ 110\mathrm{keV})$, we can take the $B(\mathrm{E1})$ from either nucleus (or an average for the two nuclei). In some cases the assumption of good isospin may not be warranted, e.g., the analog state mixes strongly with nearby states of the same J^π, and the effect on $\xi' y$ should be examined. So far we have found no cases where the effect is large enough for concern.

There is no basis [25] for a corresponding relationship between the axial matrix elements M_0^{T} and M_0^{S} although it has sometimes been assumed that M_0^{T} is related to $-M_0^{\mathrm{S}}$ as $\xi' y$ is to x. For oscillator single-particle wavefunctions with $2n + l = 2n' + l' \pm 1$

$$\langle (l\tfrac{1}{2})j \,\|i\boldsymbol{\sigma}\cdot\boldsymbol{\nabla}\|\, (l'\tfrac{1}{2})j\rangle = \mp \langle (l\tfrac{1}{2})j \,\|i\boldsymbol{\sigma}\cdot\mathbf{r}\|\, (l'\tfrac{1}{2})j\rangle / b^2 \qquad (11)$$

so that for a $1\hbar\omega$ initial state and a $0\hbar\omega$ final state,

$$M_0^{\mathrm{T}} = -M_0^{\mathrm{S}}/M_{\mathrm{N}} b^2 = -E_{\mathrm{osc}} M_0^{\mathrm{S}}, \qquad (12)$$

where E_{osc} is the energy of an oscillator quantum ($\hbar\omega$) in units of m_e. If $2\hbar\omega$ configurations are included, the relationship expressed in Eq. (12) no longer holds since the operators $\boldsymbol{\sigma}\cdot\boldsymbol{\nabla}$ and $\boldsymbol{\sigma}\cdot\mathbf{r}$ have different Hermitian conjugation properties [expressed in Eq. (11)]; contributions of $2\hbar\omega$ configurations will be constructive in one matrix element and destructive in the other. For single-particle wavefunctions other than harmonic oscillator (HO), e.g., Woods–Saxon (WS) wavefunctions, the ratio of matrix elements in Eq. (11) can be significantly state dependent with opposite effects on M_0^{S} and M_0^{T} much like the contributions of $2\hbar\omega$ configurations [5]. Thus, we shall calculate M_0^{T} directly from Eq. (6).

To summarize, we have defined six matrix elements which can be categorized by tensorial rank as

$$\begin{aligned} &\mathrm{R0}: M_0^{\mathrm{S}},\ M_0^{\mathrm{T}} \\ &\mathrm{R1}: x,\ u,\ \xi' y \\ &\mathrm{R2}: z. \end{aligned} \qquad (13)$$

We will express $\xi' y$ in terms of x via Eq. (7) so that in general there are five truly independent matrix elements contributing to a decay. In addition, there are a further three primed matrix elements $M_0^{S'}$, x', u' which, although closely related to M_0^S, x, and u, must be calculated as well.

C. Inadequacies of the Approach and Effective Operators

The operators we have just defined are subject to the usual renormalizations due to general inadequacies inherent in the restricted shell-model formalism. These are of three general types, namely nonnucleonic degrees of freedom, too restricted a model space, and inadequate radial wavefunctions. The most startling of these effects are the very large meson-exchange enhancement of the time-like component of the R0 axial current [3, 4] and the very strong quenching of unique (R2) decays due to core excitations [2]. Let us review what we know about the expected renormalizations of these operators.

1. *Nonnucleonic Effects*

A treatment of the expected effects of nonnucleonic degrees of freedom on the $R=1, 2$ beta matrix elements of $[\underline{r}, \underline{\sigma}]^R$ is not available. Blunden, Castel, and Toki [27] considered the effect on the analogous electromagnetic matrix elements and found quenching of ~ 7 % and 10 % for $R=1$ and 2, respectively. However, it is well known that nonnucleonic effects for weak and electromagnetic processes are different [13]. The meson effects on the R0 component of $[\underline{r}, \underline{\sigma}]^R$ were calculated by Towner and Khanna [24] for the $^{16}\mathrm{N}(\beta^-)^{16}\mathrm{O}\ 0^- \to 0^+$ decay and found to be generally small ($\sim$0–2 %). A general consensus of calculations of the meson enhancement of γ_5 is consistent with the value of 64 % found in a consideration of decays in light nuclei [5].

2. *Model Space Truncation*

The transitions considered herein typically take place between a state represented as $0\hbar\omega$ in the *sdpf* model space and a $1\hbar\omega$ state generated by promoting a proton through $1\hbar\omega$ and transforming it into a neutron. Our model space for this transition is complete as long as $Z \leqslant 20$, $N \geqslant 20$. For these transitions the largest expected effect arising from nucleonic contributions from outside our model space is that due to np–nh ($n=2, 4, \ldots$) excitations of both the initial and the final states. Consider the example of the $^{16}\mathrm{N}(\beta^-)^{16}\mathrm{O}\ 0^- \to 0^+$ decay shown schematically in Fig. 2. We assume initial and final states

$$|i\rangle = \sum_{m=0}^{\infty} \alpha_m |(2m+1)\,\hbar\omega\rangle; \qquad |f\rangle = \sum_{m=0}^{\infty} \alpha_m |2m\hbar\omega\rangle \tag{14}$$

and define M_{mp} as the matrix element connecting the mth initial and pth final

terms. We then have the contributions to the total matrix elements as shown in Fig. 2. We now assume a very simple model (VSM)

$$\begin{aligned} \alpha_{m+1} &= f_\alpha \alpha_m, \qquad M_{mm} = M_{00}, \\ M_{m,m+1} &= M_{01} \text{ all } m, \qquad f_1 = M_{01}/M_{00}. \end{aligned} \tag{15}$$

Then the total matrix element is

$$M = M_{00}[1 + f_\alpha f_1]. \tag{16}$$

In the $A \sim 40$ region, calculations in the mixed $(0+2)\,\hbar\omega$ model space give $f_\alpha \sim 0.5$ as was the case in the $A = 16$ calculation [5] illustrated in Fig. 2. The value of f_1 is critical. For $^{16}\mathrm{N}(\beta^-)^{16}\mathrm{O}\ 0^- \to 0^+$, a value of $f_1 \sim \pm 0.25$ was found for the R0 matrix elements with the plus sign for M_0^{S} and the minus sign for M_0^{T}. Thus, in that example the VSM gives

$$M = M_{00}[1 \pm 0.13]. \tag{17}$$

It is instructive to consider what we would have obtained in this example if we had truncated the initial and final states so that the transition was $1\hbar\omega \to (0+2)\,\hbar\omega$ or $(1+3)\,\hbar\omega \to (0+2)\,\hbar\omega$. The results for M_0^{T} would have been 0.78 and 0.74 as opposed to 0.87. The effect of core excitations is overestimated in both cases; the $1\hbar\omega \to (0+2)\,\hbar\omega$ result is somewhat closer to the VSM result than the more ambitious calculation. On the other hand consider the case in which $n\hbar\omega$ terms are negligible for $n \geq 4$; then the $(1+3)\,\hbar\omega \to (0+2)\,\hbar\omega$ result is clearly to be preferred. One thing we learn from this exercise is that one cannot generally say whether $(1+3)\,\hbar\omega \to (0+2)\,\hbar\omega$ is closer to the truth than $1\hbar\omega \to (0+2)\,\hbar\omega$. An illustration of a situation for which the VSM seems to be applicable is calculation of the unique n-forbidden beta matrix element z in the Hsieh–Mooy–Wildenthal [28] $d_{3/2}f_{7/2}$ model. Results are shown in Table I for a hypothetical $^{40}\mathrm{K}(2^-) \to {}^{40}\mathrm{Ca}(0^+)$ decay. The value of z for the full model space is in the lower right corner. It is seen that for truncation to an mp–mh initial state its value is approximated well for an

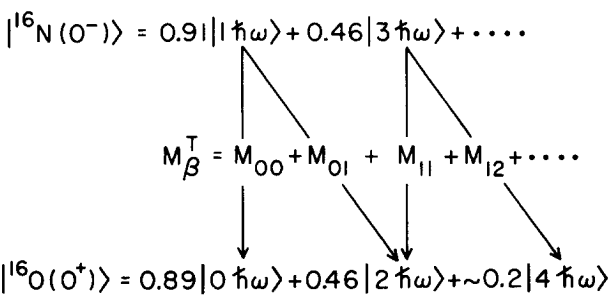

FIG. 2. Schematic of $^{16}\mathrm{N}(0^-) \to {}^{16}\mathrm{O}(0^+)\,\beta^-$ decay. The amplitudes of the various $n\hbar\omega$ components are approximate so that the wavefunctions are not quite normalized.

TABLE I

Hsieh–Mooy–Wildenthal [28] Predictions for the Unique First-Forbidden beta Matrix Element z (in fm) of Eq. (3) for a Hypothetical $^{40}K(2^-) \rightarrow {}^{40}Ca(0^+)$ Decay

Initial state ($\hbar w$)	Final state ($\hbar\omega$)				
	0	0+2	0+2+4	0+2+4+6	0+2+4+6+8
1	26.10	*15.92*	13.78	13.50	13.48
1+3	21.04	19.20	*16.86*	16.52	16.52
1+3+5	19.20	18.50	16.98	*16.64*	16.62
1+3+5+7	19.04	18.44	16.94	16.62	*16.58*

Note. The calculation was made with harmonic oscillator wavefunctions with a length parameter of 1.963 fm. The model space is eight nucleons in a $d_{3/2}f_{7/2}$ model space with the indicated np–nh components. The highlighted values are those for which the final state wavefunction contains only those terms which can connect to the indicated initial state. The near constancy of these highlighted values is to be noted and suggests that only the $1\hbar\omega \rightarrow (0+2)\,\hbar\omega$ calculation need be done.

$(m+1)$p–$(m+1)$h final state; i.e., $1\hbar\omega \rightarrow (0+2)\,\hbar\omega$ does considerably better than $(1+3)\,\hbar\omega \rightarrow (0+2)\,\hbar\omega$.

Because of the large model space dimensions involved it is not possible to make a general study of the effects of core excitations near $A=40$ without resorting to perturbative approaches. However, the archetypical case of 1p–1h excitations in ^{40}K decaying to the ^{40}Ca ground state can be handled in a large enough basis to be informative. Thus, we have calculated hypothetical 0^-, 1^-, and 2^- decays of ^{40}K to $^{40}Ca\ 0^+$ in a $1\hbar\omega \rightarrow (0+2)\,\hbar\omega$ model using the full *sdpf* model space. We find quite small departures from the $1\hbar\omega \rightarrow 0\hbar\omega$ results for R0 and R1 decays and the large effects found formerly [see Section F.1] for the R2 decay. The small effect for R0 and R1 can be traced to small matrix elements for $1\hbar\omega \rightarrow 2\hbar\omega$ which appear to result from the dominance of $f_{7/2}$ orbits in the $2\hbar\omega$ wavefunction; i.e., this orbit cannot contribute to the R0 and R1 decays while, on the other hand, $d_{3/2} \leftrightarrow f_{7/2}$ transitions dominate the R2 decays. The effect on the R1 decays appears to be small but unpredictable; that on the R0 decays is to slightly increase M_0^S and decrease M_0^T.

3. *Radial Wavefunctions*

Calculation of beta-decay matrix elements is usually performed with harmonic oscillator (HO) radial wavefunctions. Realistic radial wavefunctions can differ significantly from harmonic oscillators especially when the valence nucleons are loosely bound as is often the case in the $1\hbar\omega$ states encountered in first-forbidden beta decay. To illustrate the expected effect of using harmonic oscillators, consider

the first-order expansion of the nuclear radial wavefunctions in terms of oscillators for a single-particle $2s_{1/2} \rightarrow 1p_{1/2}$ transition,

$$|2s\rangle = |2s\rangle_{\mathrm{HO}} + \alpha_1 |1s\rangle_{\mathrm{HO}} + \alpha_2 |3s\rangle_{\mathrm{HO}} \cdots \tag{18a}$$

$$|1p\rangle = |1p\rangle_{\mathrm{HO}} + \beta_1 |2p\rangle_{\mathrm{HO}} + \beta_2 |3p\rangle_{\mathrm{HO}} \cdots; \tag{18b}$$

then, to *first order*,

$$\begin{aligned} \langle 2s| r |1p\rangle &= \langle 2s| r |1p\rangle_{\mathrm{HO}} + \alpha_1 \langle 1s| r |1p\rangle_{\mathrm{HO}} + \beta_1 \langle 2s| r |2p\rangle_{\mathrm{HO}} \\ &= (1 + y) \langle 2s| r |1p\rangle_{\mathrm{HO}}, \end{aligned} \tag{19}$$

where

$$y = -(\tfrac{3}{2})^{1/2} \alpha_1 - (\tfrac{5}{2})^{1/2} \beta_1. \tag{20}$$

The main deficiency of the harmonic oscillator wavefunctions is that the asymptotic region (large r) is relatively too small. This is remedied by adding first-order terms with negative coefficients since the sign of the asymptotic wavefunction oscillates with the principal quantum number. Thus, we expect y to be positive for the matrix element of r (and thus M_0^{S}). On the other hand, $E_f - E_i$ is positive for the zeroth-order term and negative for the first-order terms of Eq. (19). Thus, from Eqs. (11) and (12), we expect y for M_0^{T} to be the negative of y for M_0^{S}. This example illustrates that, in first order, using harmonic oscillator radial wavefunctions is expected to cause the same $(1 \pm y)$ effect on the matrix elements M_0^{S} and M_0^{T} as was found [24] for core excitations [see Eq. (16)]. Of course, calculations carried to higher order can differ significantly from this example just as they can for core excitations.

The calculation of the first-forbidden matrix elements using Woods–Saxon radial wavefunctions has been discussed fully for the $A = 16$ region [5, 6, 10]. These calculations are done by transforming to the relative coordinate system for, e.g., a $\nu \rightarrow \pi \beta^-$ transition outside an $A - 1$ core and using the appropriate separation energy for each of the first 5–10 most important core states as determined from and combined with the associated spectroscopic amplitudes. It was found that the R0 matrix elements are very sensitive to the radial wavefunctions and the evaluation of the decay rate with Woods–Saxon wavefunctions can differ by factors of 2–3 from the HO value. It was also found that the R1 and R2 matrix elements near $A = 16$ are much less sensitive to the radial form of the wavefunctions than is R0. Regardless of the radial wavefunctions used it is imperative that the associated parameters are such as to give the correct (experimental) rms size of the nucleus and comparisons between calculations done with HO and WS wavefunctions are only meaningful if they imply the same rms size of the nucleus. We belabor this point because two studies have been presented [29, 30] which purport to show considerably less sensitivity to the form of the radial wavefunctions than that found in the studies of Millener, Warburton, and collaborators [5, 6, 10]. The dis-

crepancy is due to the fact that in these two studies the HO and WS wavefunctions were not constrained to give the same nuclear radius.

Our tests of the effect of the form of the radial wavefunctions on the decay rates for $A \sim 40$ nuclei were done with both Woods–Saxon and Hartree–Fock wavefunctions. The translation to a relative coordinate system was neglected (the error introduced goes as $\sim A^{-1}$) and a single $A-1$ core was assumed. These approximations are adequate for assessing the effect. For $A \sim 40$ we find the same insensitivity for R1 and R2 and much less sensitivity for R0 than that near $A = 16$. The general effect on M_0^{S} and M_0^{T} near $A = 40$ is to increase the former by $\sim$5–10 % and decrease the latter by the same amount. The different behavior of the R0 matrix elements near $A = 16$ and 40 is due to the different sensitivities of the major components which are $2s_{1/2} \leftrightarrow 1p_{1/2}$ for $A \sim 16$ and $2p_{3/2} \leftrightarrow 1d_{3/2}$ for $A \sim 40$.

4. *Summary*

This preamble is designed to indicate the problems which need to be studied in order to understand the renormalizations of first-forbidden operators. It is also a justification for our choices of effective operators to use in the predictions of unobserved decays.

We define effective operators

$$M_{\mathrm{eff}} = q_{\mathrm{eff}} M_{\mathrm{shell\ model}}.$$

For M_0^{T} and M_0^{S} we shall take $q_{\mathrm{T}} = 0.9\varepsilon_{\mathrm{mec}}$ and $q_{\mathrm{S}} = 1.1$ where the factors 0.9 and 1.1 are a rough representation of the effects of using harmonic oscillator wavefunctions and of neglecting core excitations. We attempt some evaluation of $\varepsilon_{\mathrm{mec}}$—the meson-exchange enhancement factor—in Section F but in our predictions of unobserved decays we assume the best current value [5] of $\varepsilon_{\mathrm{mec}} = \sim 1.64$ and take $q_{\mathrm{T}} = 1.5$. Because of rather complete ignorance, we shall abide with $q_x = q_u = 1.0$ for the R1 matrix elements. The best value of q_z for the R2 decays is obtained by comparison to experiment (Section F), $q_z = 0.510$.

D. The Decay Rate

1. *Definitions and Construction*

For historical reasons, comparison between theory and experiment of the absolute decay rate for first-forbidden transitions utilizes the expression [19, 21]

$$ft = 6166 \text{ sec}, \tag{21}$$

where t is the partial half-life of the transition and

$$f = \int_1^{W_0} C(W)\, F(Z, W)(W^2 - 1)^{1/2}\, W(W_0 - W)^2\, dW. \tag{22}$$

The integrated Fermi function, f, is related to the decay rate Λ by

$$\Lambda\,(\sec^{-1}) = 1/\tau = \ln 2/t = f/8896. \tag{23}$$

In Eq. (22), W is the β energy and W_0 the disintegration energy (maximum β energy), both in units of the electron rest mass (and including the rest mass), and Z is the charge of the final nucleus. We use natural units $\hbar = c = m_e = 1$. The unit of time is seconds, and of length the electron Compton wavelength, $\lambda\!\!\!^{-}_{Ce} = 386.159$ fm. Retaining the dominant terms discussed in Section B, Schopper [19] expressed the shape factor as

$$C(W) = K + \mathrm{Ka}\,W + \mathrm{Kb}/W + \mathrm{Kc}\,W^2. \tag{24}$$

The coefficients K, Ka, Kb, Kc in Eq. (24) have small energy dependences via the functions μ_1 and λ_2 defined and tabulated, for instance, by Behrens and Jänecke [31]. For light nuclei μ_1 differs negligibly from unity except for transitions with energies higher than those encountered experimentally. Likewise, λ_2 differs negligibly from unity except for very low or high energy transitions. Although the energy dependence of μ_1 and λ_2 is not negligible in some applications, its effect on the decay rate is negligible for all observable first-forbidden decays we have encountered for $Z \leqslant 50$. We shall take $\mu_1 = \lambda_2 = 1$ in which case we can display the separation of the shape factor into rank by defining

$$C(W) = \sum_{N,R} K(NR)\,W^N \tag{25}$$

with the $K(NR)$ being independent of W and N taking on the values 0, 1, -1, 2. The equivalence to Schopper's notation is

$$K = \sum_R K(0R), \qquad \mathrm{Ka} = \sum_R K(1R), \qquad \text{etc.} \tag{26}$$

We now define the integrals, I_N, as

$$I_N = \int_1^{W_0} W^N F(Z, W)(W^2 - 1)^{1/2}\,W(W_0 - W)^2\,dW \tag{27}$$

and separate f according to rank:

$$f = \sum_R f^{(R)} = f^{(0)} + f^{(1)} + f^{(2)}. \tag{28}$$

Then

$$f^{(R)} = \sum_N K(NR)\,I_N, \qquad f = \sum_{RN} K(NR)\,I_N. \tag{29}$$

Following the treatment of Behrens and Buhring [14], we have

$$\text{R0: } K(00)=\zeta_0^2+\tfrac{1}{9}(M_0^S)^2, \qquad K(-10)=-\tfrac{2}{3}\mu_1\gamma_1\zeta_0 M_0^S \tag{30a}$$

$$\begin{aligned}\text{R1: } K(01)&=[\zeta_1^2+\tfrac{1}{9}(x+u)^2-\tfrac{4}{9}\mu_1\gamma_1 u(x+u)+\tfrac{1}{18}W_0^2(2x+u)^2-\tfrac{1}{18}\lambda_2(2x-u)^2]\\ K(11)&=-\tfrac{4}{3}uY-\tfrac{1}{9}W_0(4x^2+5u^2)\\ K(-11)&=\tfrac{2}{3}\mu_1\gamma_1\zeta_1(x+u)\\ K(21)&=\tfrac{1}{18}[8u^2+(2x+u)^2+\lambda_2(2x-u)^2]\end{aligned} \tag{30b}$$

$$\begin{aligned}\text{R2: } K(02)&=\tfrac{1}{12}z^2(W_0^2-\lambda_2),\\ K(12)&=-\tfrac{1}{6}z^2W_0,\\ K(22)&=+\tfrac{1}{12}z^2(1+\lambda_2),\end{aligned} \tag{30c}$$

where we have chosen to display the dependence on μ_1 and λ_2. (Note however that Eq. (25) is not correct if μ_1 and λ_2 are functions of W.) In Eq. (30) we have

$$\begin{aligned}V&=M_0^T+\xi M_0^{S'}, & \zeta_0&=V+\tfrac{1}{3}M_0^S W_0,\\ Y&=\xi' y-\xi(u'+x'), & \zeta_1&=Y+\tfrac{1}{3}(u-x)W_0.\end{aligned} \tag{31}$$

The coefficients $K(NR)$ depend on the nuclear matrix elements, on W_0, and on $\xi=\alpha Z/2r_u$. The parameter γ_1 is given by $[1-(\alpha Z)^2]^{1/2}$ where α is the fine structure constant. The relationships given here hold for $\beta^{\mp}$ decay with the convention that $\pm Z$ is taken in $\beta^{\mp}$ decay. The corresponding formalism for electron capture—derived from the results presented by Bambynek *et al.* [32]—is given in a recent study of ^{44}Ti(EC)^{44}Sc by Alburger and Warburton [33].

2. *Units*

We have used natural units throughout up to this point. Although it is not the elegant thing to do, there are two reasons why we would rather present the matrix elements in units of fm: (1) they are then of order unity rather than of order $\lambda\!\!\!^{-}_{Ce}^{-1}$ and (2) there are historical reasons concerning the definition of the unique first-forbidden decay rate. To accommodate this change we simply divide the I_N of Eq. (27) by $\lambda\!\!\!^{-}_{Ce}^{2}$ and multiply the matrix elements by $\lambda\!\!\!^{-}_{Ce}$ so that Eqs. (21)–(31) still apply. We note that this procedure does not give the proper units for the relativistic matrix elements and so one should think of $\lambda\!\!\!^{-}_{Ce}$—in this application—as a simple scaling factor.

E. Some Useful Definitions and Approximations

1. *Unique First-Forbidden Decays*

For $\Delta J=2$ only R2 contributes and thus there is only one nonzero matrix element; hence these decays are called unique first forbidden. From Eq. (30c) we

can find the unique first-forbidden shape factor associated with the present formalism,

$$C(W)_{\text{unique}} = \tfrac{1}{12}z^2[q^2 + \lambda_2 p^2], \tag{32}$$

where q and p are the neutrino and electron momenta, respectively. We often use a definition of unique first-forbidden transition strength which is related to that for allowed decay. That is, for allowed Gamow–Teller ($n = 0$) or unique first-forbidden decay ($n = 1$), comparison to theory can be made via the transition strength (matrix element squared), which we define as [1]

$$B_n = 6166 \left\{ \frac{[(2n+1)!!]^2}{(2n+1)} \right\} \lambda_{\text{Ce}}^{2n} (f_n t)^{-1}. \tag{33}$$

Equation (33) gives

$$B_0 = 6166/f_0 t, \qquad 10^{-6} B_1 = 2758/f_1 t \text{ fm}^2, \tag{34}$$

where f_0 and f_1 are Fermi functions calculated with shape factors of unity and $(q^2 + \lambda_2 p^2)$, respectively. In previous treatments, a unique first-forbidden transition strength $\langle G_1 \rangle^2$ has been used [1, 2]. z^2 is related to B_1 and $\langle G_1 \rangle^2$ by

$$z^2 = 4B_1 = 4\lambda^2 \langle G_1 \rangle^2. \tag{35}$$

2. *The Small Z Approximation*

If we explicitly use the approximations $\gamma_1 = \mu_1 = \lambda_2 = 1$, the coefficients of Eq. (30) simplify considerably. Thus, with these approximations, Eqs. (30) become

$$\text{R0: } K(00) = \zeta_0^2 + \tfrac{1}{9}(M_0^{\text{S}})^2, \qquad K(-10) = -\tfrac{2}{3}\zeta_0 M_0^{\text{S}} \tag{36a}$$

$$\begin{aligned} \text{R1: } K(01) &= \xi_1^2 + \tfrac{1}{18} W_0^2 (2x+u)^2 - \tfrac{1}{18}(7u^2 + 2x^2) \\ K(11) &= -\tfrac{4}{3} uY - \tfrac{1}{9} W_0 (4x^2 + 5u^2) \\ K(-11) &= \tfrac{2}{3}\xi_1 (x+u) \\ K(21) &= \tfrac{1}{18}(10u^2 + 8x^2) \end{aligned} \tag{36b}$$

$$\begin{aligned} \text{R2: } K(02) &= \tfrac{1}{12} z^2 (W_0^2 - 1) \\ K(12) &= -\tfrac{1}{6} z^2 W_0 \\ K(22) &= +\tfrac{1}{6} z^2. \end{aligned} \tag{36c}$$

3. *A Useful Approximation for the Rank 0 Contribution*

It is useful to know that the R0 contribution has very nearly the allowed shape. That is, we see from Eq. (27) that aside from very small correction factors I_0 is the Fermi integral, f_0, that occurs in Fermi or Gamow–Teller allowed decays. The R0

contribution to f comes from $K(00)$ and from the $1/w$ term, $K(-10)$, but in all practical cases

$$|\tfrac{2}{3}\mu_1\gamma_1\zeta_0 M_0^S| \ll \zeta_0^2 + \tfrac{1}{9}(M_0^S)^2 \tag{37}$$

so that usually within a few percent accuracy the $1/w$ term can be neglected. A minor consequence of this is that $\log f_0 t$ values are more meaningful for pure R0 decays such as $0^+ \leftrightarrow 0^-$ decays than for $\Delta J > 0$ first-forbidden decays.

In any practical case, the two terms in the $K(00)$ of Eq. (36a) are of disparate magnitude, i.e.,

$$\tfrac{1}{9}(M_0^S)^2 \ll \zeta_0^2. \tag{38}$$

Thus, using Eq. (31), we have the useful approximation

$$f^{(0)} \simeq I_0[M_0^T + a(Z, W_0, r_u)\, M_0^S]^2, \tag{39}$$

where

$$a(Z, W_0, r_u) = r'_w \xi + \tfrac{1}{3} W_0 \tag{40}$$

with $r'_w = M_0^{S\prime}/M_0^S \simeq 0.7$. For ease of comparison to experiment, it is useful to define a R0 beta transition strength, $B_1^{(0)}$, and an analogous composite matrix element, $M_1^{(0)}$, such that

$$B_1^{(0)} = (M_1^{(0)})^2 = [M_0^T + a(Z, W_0, r_u)\, M_0^S]^2; \tag{41}$$

then the experimental matrix element from Eq. (39) is

$$M_1^{(0)}(\text{expt}) = [f_{\text{expt}}^{(0)}/I_0]^{1/2} \tag{42}$$

and the predicted and experimental rates are conveniently compared via the $M_1^{(0)}$ of Eqs. (41) and (42). Although we shall usually use the full expression for $f^{(0)}$ in our calculations, we shall often use Eqs. (41) and (42) in our attempts to understand the underlying nuclear structure in R0 decays.

4. *Definition of an* R0 *Single-Particle Rate*

Before considering individual $\Delta J = 0$ decays it is instructive to consider some single-particle estimates which provide orientation as to what might be expected. The simplest first-forbidden $0^- \to 0^+$ transition is a 1p–1h $\to$ vac transition, and so we are interested in matrix elements for M_0^S of the type

$$\langle \text{vac} \,\|\text{ir}[C_1, \boldsymbol{\sigma}]^0 \boldsymbol{\tau}\|\, (j_f^{-1} j_i)_{0^-} \rangle. \tag{43}$$

Recalling that $M_0^T = -E_{\text{osc}} M_0^S$ for a single-particle transition evaluated with harmonic osciallator wavefunctions, we have

$$M_1^{(0)}(\text{s.p.}; j_i j_f) = [q_S a(Z, W_0, r_u) - q_T E_{\text{osc}}]\, M_0^S(\text{s.p.}; j_i j_f), \tag{44}$$

TABLE II

Single-Particle Estimates for the $\Delta J = 0$ β^- Matrix Element $M_S^{(0)}$ as Defined in Eq. (45)

A	j_i	j_f	$\lvert\frac{1}{2}\xi - E_{osc}\rvert$	$\frac{M_0^S(\text{s.p.})}{iC_A b}$	$-iM_0^S(\text{s.p.})$	$\lvert M_1^{(0)}(\text{s.p.})\rvert$
16	$2s_{1/2}$	$1p_{1/2}$	24.356	$-\sqrt{2}$	−3.1523	77
	$1d_{3/2}$	$1p_{3/2}$		$+\sqrt{10}$	+7.0487	172
40	$2p_{3/2}$	$1d_{3/2}$	17.893	-2	−4.9469	89
	$1f_{5/2}$	$1d_{5/2}$		$+\sqrt{21}$	+11.3347	203
	$2p_{1/2}$	$2s_{1/2}$		$+\sqrt{5}$	+5.5308	99
96	$3s_{1/2}$	$2p_{1/2}$	11.907	-2	−5.5242	66
	$2d_{3/2}$	$2p_{3/2}$		$+\sqrt{14}$	+10.3349	123
	$2d_{5/2}$	$1f_{5/2}$		$-\sqrt{6}$	−6.7658	81
	$1g_{7/2}$	$1f_{7/2}$		$+6$	+16.5726	198

where s.p. stands for single particle, and we have explicitly inserted the scaling factors which relate the shell-model (impulse approximation) values for M_0^S and M_0^T to the effective values (see Section C). For simplicity, we specialize to β^- transitions in neutron-rich nuclei. In the evaluation of Eq. (44) we shall take $W_0 = E_{osc} - r'_w \xi$ and $r'_w = 0.70$. We then arbitrarily approximate q_S and $q_T \simeq 1.07$ and $q_T \simeq 1.36$ which results in a simple expression for our single-particle estimate:

$$M_1^{(0)}(\text{s.p.}; j_i j_f) \cong [\tfrac{1}{2}\xi - E_{osc}]\, M_0^S(\text{s.p.}; j_i j_f). \tag{45}$$

In Table II we list results for transitions of this type encountered at $A = 16$, 40, and 96. These values of A were used in the evaluations of $\hbar w$, b, and r_u necessary to the evaluation of Eq. (45). A criterion used in the evaluation of nuclear data by the International Network For Nuclear Structure Evaluation is that a beta transition is allowed if $\log f_0 t < 5.9$—see, e.g., [34]. This criterion is based on the compilation of Raman and Gove [35]. From Eqs. (21) and (39) we can deduce that $M_1^{(0)} < 34$ fm corresponds to $\log f_0 t > 5.9$. From Table II it is seen that this limit is generously exceeded by the single-particle estimates. In actual fact, some $J \to J$, $\pi_i \pi_f = -$, transitions (but no first-forbidden $\Delta J > 0$ transitions) do have experimental values of $\log f_0 t < 5.9$. For instance the $^{16}\text{N}(0^-) \to {}^{16}\text{O}(0^+)$ and $^{96}\text{Y}(0^-) \to {}^{96}Zr(0^+)$ decays have $\log f_0 t = 5.53$ and 5.61, respectively. Thus the accepted limit dividing first-forbidden and allowed beta transitions is in need of revision.

F. Comparison to Experiment

Experimental information on the known first-forbidden decays in $A = 37$–44 nuclei is collected in Tables III and IV. The unique first-forbidden beta transition

TABLE III

Unique First-Forbidden Beta Decays in $A = 35$–44 Nuclei[a]

Transition	$J_i^\pi; T_{zi}$	$J_f^\pi; T_{zf}$	E_x (keV)	Half-life (sec)	Branch (%)	Q (keV)	Refs.	B_1(expt) (fm^2)	B_1(WBMB) (fm^2)
^{37}S(β^-)^{37}Cl	$\frac{7}{2}^-; \frac{5}{2}$	$\frac{3}{2}^+; \frac{3}{2}$	0	3.030 (12) [+2]	5.6 (6)	4865.16 (24)	*b*	1.32 (14)	6.170
^{38}S(β^-)^{38}Cl	$0^+; 3$	$2^-; 2$	0	1.022 (42) [+4]	12.7 (32)	2936 (12)	*b*	2.12 (54)	7.992
^{38}Cl(β^-)^{38}Ar	$2^-; 2$	$0^+; 1$	0	2.234 (3) [+3]	57.6 (13)	4916.5 (8)	*b*	1.67 (4)	6.126
^{39}Cl(β^-)^{39}Ar	$\frac{3}{2}^+; \frac{5}{2}$	$\frac{7}{2}; \frac{3}{2}$	0	3.336 (12) [+3]	7.0 (20)	3438 (18)	*c*	1.3 (4)	4.328
^{39}Ar(β^-)^{39}K	$\frac{7}{2}^-; \frac{3}{2}$	$\frac{3}{2}^+; \frac{1}{2}$	0	8.49 (9) [+9]	100.0	565 (5)	*d*	0.221 (11)	0.553
^{40}Cl(β^-)^{40}Ar	$2^-; 3$	$0^+; 2$	0	8.10 (12) [+1]	9.0	7513 (35)	*e, f, g, h*	0.45	3.215
^{40}Cl(β^-)^{40}Ar		$4^+; 2$	2893		0.5 (2)	4620 (35)	*e, f, g, h*	0.59 (23)	1.655
$^{40}K(EC)^{40}$Ar	$4^-; 1$	$2^+; 2$	1461	4.027 (25) [+16]	10.67 (11)	44.0 (17)	*d, i*	0.0079 (15)	0.0132
^{41}Ar(β^-)^{41}K	$\frac{7}{2}^-; \frac{5}{2}$	$\frac{3}{2}^+; \frac{3}{2}$	0	6.576 (24) [+3]	0.83 (8)	2492.3 (7)	*d, j*	0.56 (4)	1.639
^{41}Ca(EC)^{41} K	$\frac{7}{2}^-; \frac{1}{2}$	$\frac{3}{2}^+; \frac{3}{2}$	0	2.43 (35) [+12]	100.0	421.3 (4)	*d, j*	0.108 (16)	0.164
^{42}Cl(β^-)^{42}Ar	$(2^-); 4$	$0^+; 3$	0	6.9 (3)	20.0	10000 (200)	*g, h, k*	1.79	0.658
^{42}Cl(β^-)^{42}Ar		$(0^+); 3$	2512		0.12	7488 (200)	*g, h, k*	0.072	*l*
^{42}Cl(β^-)^{42}Ar		$4^+; 3$	3096		1.52	6904 (200)	*g, h, k*	1.56	0.954
^{42}Ar(β^-)^{42}K	$0^+; 3$	$2^-; 2$	0	1.04 (3) [+9]	100.0	600 (40)	*d, j*	1.34 (40)	3.427
^{42}K(β^-)^{42}Ca	$2^-; 2$	$0^+; 1$	0	4.450 (1) [+4]	81.2 (6)	3525.1 (12)	*i, j*	0.901 (9)	4.668
^{42}K(β^-)^{42}Ca		$0^+; 1$	1837		0.35 (3)	1687.8 (13)	*i, j*	0.33 (3)	*l*
^{43}K(β^-)^{43}Ca	$\frac{3}{2}^+; \frac{5}{2}$	$\frac{7}{2}^-; \frac{3}{2}$	0	8.03 (36) [+4]	1.54 (18)	1817 (10)	*d, i, m*	0.54 (6)	1.484
^{44}K(β^-)^{44}Ca	$2^-; 3$	$0^+; 2$	0	1.328 (11) [+3]	34.0 (100)	5660 (40)	*g, i, j*	0.62 (18)	4.351
^{44}K(β^-)^{44}Ca		$0^+; 2$	1884		1.5 (2)	3776 (40)	*g, i, j*	0.36 (5)	*l*
^{44}K(β^-)^{44}Ca		$4^+; 2$	2283		0.6 (2)	3377 (40)	*g, i, j*	0.29 (10)	1.855

[a] Uncertain spin or parity assignments are in parentheses, as are the uncertainties in the least significant figure of the experimental values. The numbers in square brackets are powers of 10.

[b] Reference [17].

[c] Reference [36].

[d] Reference [2].

[e] Reference [37].

[f] Reference [38], the gamma-ray data were compiled at the National Nuclear Data Center (NNDC) and reported in Ref. [39].

[g] Other first-forbidden branches from this decaying body are known or possible. We list only those branches proceeding to final states of definite spin and parity.

[h] Branching ratio uncertainties are not given.

[i] Reference [40].

[j] Reference [41].

[k] Reference [38], the mass excess of ^{42}Cl is estimated [41].

[l] Possible intruder (see text).

[m] Reference [42].

TABLE IV

$\Delta J = 0$ and 1 First-Forbidden Beta Decays in $A = 35$–44 Nuclei[a]

Transition	$J_i^\pi; T_{zi}$	$J_f^\pi; T_{zf}$	E_x (keV)	Half-life (sec)	Branch (%)	Q (keV)	Refs.	f(expt)	f(WBMB)
					$\Delta J = 1$				
$^{37}S(\beta^-)^{37}Cl$	$\frac{7}{2}^-; \frac{3}{2}$	$\frac{5}{2}^+; \frac{3}{2}$	3086	3.030 (12) [+2]	0.040 (21)	1778.82 (30)	*b*	8.1 (43) [−3]	9.0 [−5]
$^{38}S(\beta^-)^{38}Cl$	$0^+; 3$	$(1)^-; 2$	1692	1.022 (42) [+4]	0.17 (2)	1243 (12)	*b*	1.03 (12) [−3]	0.34 [−3]
$^{43}K(\beta^-)^{43}Ca$	$\frac{3}{2}^+; \frac{5}{2}$	$\frac{5}{2}^-; \frac{3}{2}$	373	8.03 (36) [+4]	0.9 (6)	1444 (10)	*c, d, e*	7 (5) [−4]	2.5 [−4]
$^{44}Ti(EC)^{44}Sc$	$0^+; 0$	$1^-; 1$	68	2.11 (3) [+9]	0.7 (3)	198.5 (21)	*f, g, h*	2.6 (9) [−8]	1.06 [−7]
					$\Delta J = 0$				
$^{38}S(\beta^-)^{38}Cl$	$0^+; 3$	$(0^-); 2$	1745	1.022 (42) [+4]	2.37 (11)	1191 (12)	*b*	1.43 (7) [−2]	3.81 [−2]
$^{38}Cl(\beta^-)^{38}Ar$	$2^-; 2$	$2^+; 1$	2167	2.234 (3) [+3]	10.5 (3)	2749.0 (8)	*b*	2.90 (8) [−1]	1.68 [−1]
$^{39}Cl(\beta^-)^{39}Ar$	$\frac{3}{2}^+; \frac{5}{2}$	$\frac{3}{2}^-; \frac{3}{2}$	1267	3.336 (12) [+3]	4.5 (16)	2171 (18)	*i*	0.83 (30) [−1]	1.09 [−1]
$^{40}Cl(\beta^-)^{40}Ar$	$2^-; 3$	$2^+; 2$	2524	8.10 (12) [+1]	1.8 (5)	4989 (35)	*j, k, l*	1.37 (38)	*m*
$^{41}Ar(\beta^-)^{41}K$	$\frac{7}{2}^-; \frac{5}{2}$	$\frac{7}{2}^+; \frac{3}{2}$	1677	6.576 (24) [+3]	0.052 (5)	815.1 (7)	*c, f*	4.9 (19) [−4]	2.9 [−4]
$^{42}Cl(\beta^-)^{42}Ar$	$(2^-); 4$	$2^+; 3$	1208	6.9 (3)	27.0	8792 (200)	*d, l, n*	2.41 [+2]	0.40 [+2]
$^{42}Cl(\beta^-)^{42}Ar$	$(2^-); 4$	$(2^+); 3$	2487		3.7	7513 (200)	*l, n, o*	3.31 (+1)	0.58 [+1]
$^{42}Cl(\beta^-)^{42}Ar$	$(2^-); 4$	$2^+; 3$	3558		0.14	6442 (200)	*l, n, o*	1.25	*m*
$^{42}K(\beta^-)^{42}Ca$	$2^-; 2$	$2^+; 1$	1525	4.450 (1) [+4]	18.3 (6)	2000.5 (12)	*d, f*	2.54 (8) [−2]	0.78 [−2]
$^{42}K(\beta^-)^{42}Ca$		$2^+; 1$	2424		0.05 (1)	1101.5 (12)	*d, f*	6.9 (14) [−5]	*m*
$^{43}K(\beta^-)^{43}Ca$	$\frac{3}{2}^+; \frac{5}{2}$	$\frac{3}{2}^-; \frac{3}{2}$	593	8.03 (36) [+4]	4.06 (13)	1224 (10)	*c, d, e*	3.1 (1) [−3]	0.81 [−3]
$^{44}K(\beta^-)^{44}Ca$	$2^-; 3$	$2^+; 2$	3301	1.328 (11) [+3]	0.2 (1)	2359 (40)	*d, f, l*	9.3 (47) [−3]	*m*
$^{44}K(\beta^-)^{44}Ca$		$2^+; 2$	4651		0.08 (5)	1009 (40)	*d, f, l*	3.7 (23) [−3]	*m*
$^{44}Ti(EC)^{44}Sc$	$0^+; 0$	$0^-; 1$	146	2.11 (3) [+9]	99.1 (3)	120.1 (21)	*f, g, h*	2.90 (8) [−6]	1.07 [−6]

[a] The f(WBMB) are calculated with the effective operators summarized in Section C. Uncertain spin or parity assignments are in parentheses, as are the uncertainties in the least significant figure of the experimental values. The numbers in square brackets are powers of 10.

[b] Reference [17].

[c] Reference [2].

[d] Reference [40].

[e] Reference [42].

[f] Reference [41].

[g] Reference [43].

[h] Reference [33], the calculation was performed in a truncated basis (see text).

[i] Reference [36].

[j] Reference [37].

[k] Reference [38], the gamma-ray data were compiled at the National Nuclear Data Center (NNDC) and reported in Ref. [39].

[l] Other first-forbidden branches from this decaying body are known or possible. We list only those branches proceeding to final states of definite spin and parity.

[m] Possible intruder.

[n] Branching ratio uncertaintics are not given.

[o] Reference [38], the mass excess of ^{42}Cl is estimated [41]. The calculation was performed in a truncated basis (see text).

strength, B_1, is included in Table III and $f = 6166/t$ is listed in Table IV. We note that no first-forbidden decays are known for $A = 22$–36 nuclei. We first consider the unique ($\Delta J = 2$) decays of Table III.

1. *Unique First-Forbidden Decays*

In the second and third columns of Table V we compare the experimental B_1 to predictions for the full WBMB model space using the free-nucleon operator. Not all the decays of Table III are included in this comparison. In the full WBMB model space, the 2^- states of ^{42}Cl have a J-dimension well beyond our computational capabilities. However, we consider $^{42}\mathrm{Cl}(\beta^-)^{42}\mathrm{Ar}$ in a truncated basis in Section G of this paper. The ^{42}Ca 0_2^+ state at 1837 keV and the ^{44}Ca 0_2^+ state at 1884 keV are identified as np–nh ($n = 2, 4, \ldots$) excitations and thus are outside the WBMB model space. We also consider these decays in Section G.

An examination of Table V reveals that the WBMB predictions are generally larger than experiment. This is as expected since we have not included ground-state correlations in either the initial or the final states. Towner and his colleagues [2, 44] included ground-state correlations to order $2\hbar\omega$ perturbatively and they found an average diminution of the B_1 for $A = 37$–44 nuclei of ~ 3.7. On general grounds we might expect a further quenching due to mesonic and nucleonic struc-

TABLE V

Comparison of the Experimental Unique First-Forbidden Beta Transition Strengths to the Predictions of the WBMB Interaction Calculated with the Operator Appropriate to Free Space, B_1(WBMB; free), and an Effective Operator, B_1(WBMB; eff)

Transition					
Initial state	Final state	B_1(expt) (fm^2)	B_1(WBMB; free) (fm^2)	B_1(WBMB; eff) (fm^2)	Deviation (%)
$^{37}\mathrm{S}(\frac{7}{2}^-)$	$^{37}\mathrm{Cl}(\frac{3}{2}^+)$	1.32 (14)	6.17	1.61	22.3
$^{38}S(0^+)$	$^{38}\mathrm{Cl}(2^-)$	2.12 (54)	7.99	2.09	−1.4
$^{38}\mathrm{Cl}(2^-)$	$^{38}\mathrm{Ar}(0^+)$	1.67 (4)	6.13	1.60	−4.1
$^{39}\mathrm{Cl}(\frac{3}{2}^+)$	$^{39}\mathrm{Ar}(\frac{7}{2}^-)$	1.3 (4)	4.33	1.13	−12.9
$^{39}\mathrm{Ar}(\frac{7}{2}^-)$	$^{39}\mathrm{K}(\frac{3}{2}^+)$	0.221 (11)	0.55	0.14	−34.6
$^{40}\mathrm{Cl}(2^-)$	$^{40}\mathrm{Ar}(0^+)$	0.45	3.22	0.84	86.9
$^{40}\mathrm{Cl}(2^-)$	$^{40}\mathrm{Ar}(4^+)$	0.59 (23)	1.66	0.43	−26.6
$^{40}\mathrm{K}(4^-)$	$^{40}\mathrm{Ar}(2^+)$	0.0079 (15)	0.0132	0.0035	−56.3
$^{41}\mathrm{Ar}(\frac{7}{2}^-)$	$^{41}\mathrm{K}(\frac{3}{2}^+)$	0.56 (4)	1.64	0.43	−23.4
$^{41}\mathrm{Ca}(\frac{7}{2}^-)$	$^{41}\mathrm{K}(\frac{3}{2}^+)$	0.108 (16)	0.164	0.043	−60.3
$^{42}\mathrm{Ar}(0^+)$	$^{42}\mathrm{K}(2^-)$	1.34 (40)	3.43	0.90	−32.8
$^{42}\mathrm{K}(2^-)$	$^{42}\mathrm{Ca}(0^+)$	0.901 (9)	4.67	1.22	35.5
$^{43}\mathrm{K}(\frac{3}{2}^+)$	$^{43}\mathrm{Ca}(\frac{7}{2}^-)$	0.54 (6)	1.48	0.39	−29.8
$^{44}\mathrm{K}(2^-)$	$^{44}\mathrm{Ca}(0^+)$	0.62 (18)	4.35	1.14	83.5
$^{44}\mathrm{K}(2^-)$	$^{44}\mathrm{Ca}(4^+)$	0.29 (10)	1.86	0.49	67.3

Note. All final states are yrast states.

ture effects (see Section C). In order to predict unobserved branches it is desirable to define effective first-forbidden operators which take account of such effects in as accurate a manner as possible. For the unique decays this is a strightforward task. We define an effective rank 2 operator for the WBMB model space by

$$z_{\text{eff}} = q_z z \tag{46}$$

and evaluate q_z^2 as the average value of $B_1(\text{expt})/B_1(\text{WBMB})$. For the data of Table V, this procedure gives $q_z = 0.510$, corresponding to a diminution of $B_1(\text{WBMB})$ of 3.84 in essentially exact agreement with the perturbative estimate [2] for the effects of ground-state correlations. The effective B_1 are listed in the fifth column of Table V while the percentage deviations of these B_1 from experiment are given in the sixth column. The structure of most of these decays was discussed by Towner *et al.* [2]. Some of the B_1 values are quite small due to cancellation effects within the WBMB model space. The consistency of the results is quite satisfactory (especially considering these cancellation effects). There is a tendency for the agreement of the effective B_1 with experiment to decrease with increasing A. We note that the WBMB interaction is well tested for $A \leqslant 41$ but this is its first application for $A > 41$. In summary, it would appear that the effects of ground-state correlations on unique decays are relatively state independent. In our calculations of nonunique decays we shall use $q_z = 0.510$ in evaluating the R2 contribution.

2. *The $\Delta J = 1$ Transitions*

As shown in Table IV, there are only four definite $\Delta J = 1$ first-forbidden transitions in the $A = 22$–44 region and for two of these the uncertainty on the branching ratio is larger than 50 % so that there is considerable doubt as to the existence of the transition at the listed strength. The predictions for all but ^{44}Ti(EC)^{44}Sc are seen to be considerably less than experiment. Can we learn anything of value about the rank 1 matrix elements from this comparison? First, we should consider the composition of the two $J_i \neq 0$ transitions. Both the ^{37}S and ^{43}K decays are predicted to have roughly equal contributions from rank 1 and rank 2. For ^{37}S the R1 contributions of x and u are predicted to be largely destructive while for ^{43}K they are predicted to be largely constructive. These facts and the large uncertainties attached to these two decay modes make it difficult to unravel the effects of the matrix elements x, u, and z on these two decays.

The predictions for the two $0^+ \to 1^-$ decays have quite different dependencies on x and u. In the ^{38}S decay the contributions of x and u add destructively. An approximate expression for f in terms of x and u can be obtained,

$$f \approx 0.070[1 - 0.181(u/x)]^2 \qquad \text{for } ^{38}\text{S}(0^+) \to {}^{38}\text{Cl}(1^-) \tag{47a}$$

and with our predictions of $x = 0.1424$ fm, $u = 0.7314$ fm we have

$$f \approx 0.070[1 - 0.93]^2 = 3.4 \times 10^{-4}. \tag{47b}$$

We see that the x and u contributions are in almost complete cancellation—only a

5 % change in the ratio of u to x is necessary to reproduce experiment so that the agreement can be considered as quite satisfactory.

The sensitivity of the ^{37}S and ^{38}S $\Delta J = 1$ decays to the radial wavefunctions was examined by calculating both decays with Woods–Saxon wavefunctions as well as with HO wavefunctions. Neither was very sensitive; the ^{37}S f-value increased by 1.0 % and the ^{38}S decay (with its nearly complete cancellation between x and u) increased by 23 %.

The ^{44}Ti $0^+ \rightarrow 1^-$ decay, being electron capture, has a particularly simple dependence on x and u [33]. To a very good approximation we can write

$$f = 3.094 \times 10^{-8}[9.203x + 4.518u]^2 \qquad \text{for } ^{44}\text{Ti}(0^+) \rightarrow {}^{44}\text{Sc}(1^-) \tag{48}$$

and, with our predictions (see Section G) of $x = 0.142$ fm, $u = 0.131$ fm we have constructive interference and thus less sensitivity to the inadequacies of the model. We note that ^{44}Ti decay and ^{42}Ti decay (see Table IX) are the only ones considered for which the model space is not complete. That is, transitions from a $0\hbar\omega$ Ti state can also occur via Sc excitations in which a neutron resides in the *gds* major shell. The effect of neglecting such excitations has been considered in a recent study of ^{44}Ti decay [33]. Unfortunately it appears that neglect of the *gds* shell renders the result of Eq. (48) all but meaningless.

3. $\Delta J = 0$ *First-Forbidden Transitions*

As for the unique ($\Delta J = 2$) decays, some of the $\Delta J = 0$ decays are to final states which we interpret as outside our model space or possibly so. These are so labelled in Table IV and will not be considered further. All but one of the remaining final states in Table IV are yrast states. The predictions for the decay to these yrast states are compared to experiment in Table VI. The method of comparison is to extract the experimental rank 0 beta transition strength $B_1^{(0)}$ defined in Section E.3 and compare it to the predicted $B_1^{(0)}$ by extracting the meson-enhancement factor ε_{mec} (Section C) necessary to give agreement; this is done with $q_{\text{T}} = 0.9\varepsilon_{\text{mec}}$ and $q_{\text{s}} = 1.1$ (see Section C). For $J \neq 0$ decays the total f-value includes contributions from rank 1 and rank 2 as well as rank 0. For these we define a rank 0 $f_{\text{expt}}^{(0)}$ as

$$f_{\text{expt}}^{(0)} = f_{\text{expt}} - f_{\text{WBMB}}^{(1)} - f_{\text{WBMB}}^{(2)}. \tag{49}$$

The accuracy of this approach depends on the relative contribution of the three ranks. As shown in the last column of Table VI, it is a viable approach because $f_{\text{expt}} \gg f_{\text{WBMB}}^{(1)} + f_{\text{WBMB}}^{(2)}$.

The expected value of ε_{mec} is ~ 1.65 [5]. The average value for the $A = 38$–41 entries of Table VI is 1.70, in good agreement with this prediction. Note that the applicability of the WBMB interaction to the $A \leqslant 41$ region has been well tested so that this agreement is gratifying. As remarked earlier, the WBMB interaction has not been tested previously for $A \geqslant 42$ nuclei. The unrealistically large values of ε_{mec}

TABLE VI

Comparison of the Predicted and Experimental $\Delta J = 0$ Matrix Elements $M_1^{(0)}$ of Eq. (42) via the Meson-Exchange Factor ε_{mec}

Transition						
Initial state	Final state	$M_1^{(0)}(\text{expt}) = [f_{\text{expt}}^{(0)}/I_0]^{1/2}$	$0.9.M_0^T$	$-1.1 \cdot a(Z, w_0, r_u) \cdot M_0^S$	ε_{mec}	$(f^{(1)}+f^{(2)})/f_{\text{expt}}$ (%)
$^{38}S(0^+)$	$^{38}Cl(0^-)$	11.8 (6)	13.90	3.94	1.13	0
$^{38}Cl(2^-)$	$^{38}Ar(2^+)$	8.96 (23)	7.72	1.85	2.10	4.1
$^{39}Cl(\frac{3}{2}^+)$	$^{39}Ar(\frac{3}{2}^-)$	8.1 (15)	6.84	2.12	1.49	1.3
$^{41}Ar(\frac{7}{2}^-)$	$^{41}K(\frac{7}{2}^+)$	4.4 (9)	2.45	0.72	2.09	1.4
$^{42}Cl(2^-)$	$^{42}Ar(2^+)$	18.0	4.79	2.81	4.35[a]	9.0
$^{42}K(2^-)$	$^{42}Ca(2^+)$	5.2 (1)	2.00	0.52	2.86	1.2
$^{43}K(\frac{3}{2}^+)$	$^{43}Ca(\frac{3}{2}^-)$	4.5 (3)	1.86	0.58	2.73	0.6
$^{44}Ti(0^+)$	$^{44}Sc(0^-)$	15.0 (4)	7.02	1.95	2.41[a]	0

[a] Calculated in a truncated basis (see text).

for $A > 41$ in Table VI signals a lessened applicability of the WBMB interaction in this region. There is reason to question the very large ε_{mec} value obtained for the ^{42}Cl decay rate as is discussed in Section G. For the other three $A > 41$ results, the too small value of $f_{\text{WBMB}}^{(0)}$ could possibly be due to too small admixture of the $p_{3/2}$, $f_{5/2}$, and $p_{1/2}$ orbits in the (fp) part of the wavefunction; i.e., the dominant $f_{7/2}$ orbit does not contribute to the $\Delta J < 2$ first-forbidden decays.

G. Some Truncated Calculations

1. *General Considerations*

As discussed in the last section, some of the transitions of Tables III and IV involve J-dimensions in the full WBMB model space which exceed our computational resources and some involve states which are outside of the WBMB model space. In this section we describe the calculation of both of these types of transitions in truncated bases. We first consider the decays of ^{42}Cl and ^{44}Ti, both of which are of the first type. We then consider some unique decays to intruder states in a $d_{3/2}f_{7/2}$ model space.

2. $^{42}Cl(\beta^-)^{42}Ar$

The WBMB model space for the 2^- ^{42}Cl ground state is $\pi(2s, 1d)^{-3}\, \nu(1f, 2p)^5$. We shall truncate this model space by restricting the number of neutrons allowed out of the $f_{7/2}$ orbit. We follow the customary procedure of designating a truncation of $(1f, 2p)^n$ to $\leqslant m$ nucleons in all possible permutations within the $f_{5/2}$, $p_{3/2}$, $p_{1/2}$ orbits as $f_{7/2}^{n-m}r^m$. With truncation to $f_{7/2}^3 r^2$ the J-dimension is 8978. Further

truncation is necessary. We allow all $f_{7/2}^3 r^2$ for $r = p_{3/2}$ but use $f_{7/2}^4 r$ for the $f_{5/2}$ and $p_{1/2}$ orbits. This truncation produces a J-dimension of 2566. To be consistent, the ^{42}Ar model space should be truncated to $f_{7/2}^2 r^2$ for $r = p_{3/2}$ and $f_{7/2}^3 r$ for $r = f_{5/2}, p_{1/2}$. We have calculated the first-forbidden decays with the truncated ^{42}Cl model space and (1) the same truncation for ^{42}Ar and (2) the full WBMB space for ^{42}Ar. The difference between (1) and (2) provides some measure of the effect of the truncation. The unique transition strengths were calculated in the full and truncated WBMB model space using $q_z = 0.510$. The results are compared to experiment in Table VII. We also show in Table VII the results of a calculation in the highly truncated $d_{3/2} f_{7/2}$ model space of Hsieh, Mooy, and Wildenthal [28]. For the 2^- ^{42}Cl ground state the truncation is to $d_{3/2}^5 f_{7/2}^5$ while the ^{42}Ar 0_1^+ and 4_1^+ states are generated from $d_{3/2}^6 f_{7/2}^4$. The calculations of Towner *et al.* [2] in a $d_{3/2}^n f_{7/2}^m$ model space showed a similar consistency for the diminution of the unique rate to that found in the WBMB model space. Towner *et al.* found $q_z^{-2} = 7 \pm 1$ reproduced experiment quite well. The results for column (c) of Table VII were so calculated. We also show in Table VII a result for the 0_2^+ state of ^{42}Ar assuming it is the lowest state of $d_{3/2}^4 f_{7/2}^6$.

The comparison to experiment of Table VII shows that the predictions for the ^{42}Cl unique decay are in much worse agreement with experiment than the others considered in Table V. From a consideration of the results for the $d_{3/2} f_{7/2}$ model space it does not seem likely that this disagreement is due to the truncation described here. Rather we suggest there may be some difficulty with the experiment. This is hard to judge since a description of the experiment has not been published, only the results without uncertainties.

Another indication of some difficulty—either theoretically or experimentally—is that the prediction for the R0 ^{42}Cl$(2^-) \rightarrow$ ^{42}Ar(2_1^+) rate falls short of experiment more than any other decay in Table VI. We note that all R0 and R1 rates are

TABLE VII

Comparison of Predicted and Experimental Unique First-Forbidden Decays in ^{42}Cl$(2^-) \rightarrow$ ^{42}Ar(J_n^π)

Final state J_n^π	B_1(fm^2)			
	[a]	[b]	[c]	Expt
0_1^+	0.17	0.16	0.33	1.79
0_2^+	[d]	[d]	0.04	0.072
4_1^+	0.25	[e]	0.85	1.56

[a] Truncated WBMB basis for ^{42}Ar.

[b] Full WBMB basis for ^{42}Ar.

[c] $d_{3/2}^n f_{7/2}^{10-n}$ model space with $n = 5$ for the ^{42}Cl 2^- state, $n = 6$ for the ^{42}Ar 0_1^+ and 4_1^+ states, and $n = 4$ for the ^{42}Ar 0_2^+ state. $q_z^{-2} = 7$ was used for all three final states.

[d] Outside the model space.

[e] The calculation was not done.

identically zero in a $d_{3/2} f_{7/2}$ model space. Thus, we do not consider the ^{42}Cl decays to the 2_n^+ states with $n > 2$ since these states are quite possibly intruders in the WBMB model space.

3. ^{44}Ti$(EC)^{44}$Sc

In a full (*sdpf*) space, the decay of ^{44}Ti, in lowest order, would involve

$$(2s, 1d)^{24} (1f, 2p)^4 \rightarrow (2s, 1d)^{23} (1f, 2p)^5. \tag{50}$$

The ^{44}Sc 0^- and 1^- wavefunctions corresponding to the model space on the right in Eq. (50) have J-dimensions of 6151 and 17530, respectively. These exceed our computational resources and some model space truncation is necessary in order to estimate these decay rates. The truncation chosen was to restrict the $(1f, 2p)^5$ space by demanding at least three $f_{7/2}$ nucleons with the remaining two distributed freely among the four *fp* orbits, this we term an $f_{7/2}^3 r^2$ space. With this restriction the J-dimensions become 1370 and 3956, respectively. The dimensions of the $J^\pi = 0^+$ states in the full $(1f, 2p)^4$ space for the $(J, T) = (0, 0)$ and $(2, 1)$ states are only 66 and 285, respectively. However, to be consistent in the calculation of EC and γ rates the $(1f, 2p)^4$ model space should also be truncated. Since the electron capture transitions involve $\pi(s, d) \rightarrow \nu(fp)$, the analogous truncation is to $f_{7/2}^3 r$ which was used and is shown in Tables IV and VI. However, the calculation of the decays was repeated with no truncation and truncation to $f_{7/2}^2 r^2$ for ^{44}Ti. For these calculations the $0^+ \rightarrow 0^-$ M_0^S matrix element differed from the result for the $f_{7/2}^3 r$ truncation by -18 and -9 %, respectively. The remarks as to the inadequacy of the shell-model space used for the ^{44}Ti R1 decay [Section F.2] hold for this R0 decay as well.

4. *Unique Decays to 2p–2h 0^+ States*

We have already discussed the decay of the 2^- ^{42}Cl ground state to the first 2p–2h intruder state of ^{42}Ar which we identify as the 0_2^+ state at 2512 keV. There are similar decays listed in Table III for ^{42}K$(\beta^-)^{42}$Ca and ^{44}K$(\beta^-)^{44}$Ca. For both Ca isotopes we identify the 0_2^+ state as a 2p–2h intruder. The question we ask here is whether or not a $(1+3)\hbar\omega \rightarrow (0+2+4)\hbar\omega$ $d_{3/2}^n f_{7/2}^m$ calculation in a $d_{3/2} f_{7/2}$ model space can reproduce the relative beta transition strengths for 0_2^+ and 0_1^+ in

TABLE VIII

The Ratio of Unique First-Forbidden Beta Transition Strengths for Decay of 2^- States to the First Two 0^+ States of ^{42}Ar, ^{42}Ca, and ^{44}Ca

		$B_1(0_2^+)/B_1(0_1^+)$	
Decay	Expt	$(1+3)\hbar\omega \rightarrow (0+2+4)\hbar\omega$	$(1+3)\hbar\omega \rightarrow (0+2)\hbar\omega$
^{42}Cl$(\beta^-)^{42}$Ar	0.04	0.04	0.12
^{42}K$(\beta^-)^{42}$Ca	0.37	0.44	0.08
^{44}K$(\beta^-)^{44}$Ca	0.58	0.25	0.08

these three nuclei. Comparison to experiment is made in Table VIII. It is seen that the Hsieh–Mooy–Wildenthal [28] $d_{3/2}f_{7/2}$ model in the $(1+3)\hbar\omega \rightarrow (0+2+4)\hbar\omega$ model space does a very creditable job of explaining the relative rates and does much better than $(1+3)\hbar\omega \rightarrow (0+2)\hbar\omega$.

H. Predictions for Unobserved Transitions

In this section we present predictions for unobserved first-forbidden transitions. One motive is to provide estimates of the effect on allowed beta branching decay rates of any significant but overlooked first-forbidden branches. Another motive is to identify those cases worthy of future study. We use the effective operators discussed in Section C for predictions. Results for $A = 35$–44 nuclei are collected in Table IX.

The quantities listed in Table IX are defined as follows:

Q_0: The mass difference between parent and daughter.

$t_{1/2}$(total): The experimental half-line of the parent.

$t_{1/2}$(FFB): The predicted partial half-line for first-forbidden beta decay calculated for all energetically accessible decays.

BR(FFB): The percentage of decays predicted to be first-forbidden; $\text{BR(FFB)} = 100 \cdot t_{1/2}(\text{total})/t_{1/2}(\text{FFB})$.

br(FFB): The percentage of first-forbidden intensity predicted to proceed via the level in question.

br(total): The predicted total branching ratio for the level in question; $\text{br(total)} = 0.01 \cdot \text{br(FFB)} \cdot \text{BR(FFB)}$.

br(expt): The experimental branching ratio information (if known).

We omit from consideration here those nuclei which have been treated adequately in previous sections. These include the decays of ^{37}S, ^{38}S, ^{38}Cl, and ^{42}Cl. For the $A = 35$–38 nuclei of Table IX there are no known first-forbidden decays. The only branch in this group predicted to be greater than 1 % is ^{36}P decay to ^{36}S 2_1^+. This branch would be difficult to measure accurately because of γ cascades from higher levels [46]. The one discrepancy in the $A = 35$–38 nuclei is the ^{37}K R0 branch to $\frac{3}{2}_1^-$. A further search for this branch would be of interest.

The potentially most interesting decay in the table is the $^{38}\text{Ca}(\beta^+)^{38}\text{K}\ 0^+ \rightarrow 0^-$ transition which has the very small predicted $\log f_0 t$-value of 5.52. A determination of this branch—predicted to be 0.03 %—would be of considerable interest because of its value in the study of meson enhancement of R0 decays. We have not previously discussed a $0^+ \rightarrow 0^-$ β^+ decay, and therefore we consider this decay in more detail. In the β^- R0 decays considered so far we have $1\hbar\omega \rightarrow 0\hbar\omega$ transitions so that M_0^{T} has the opposite sign from M_0^{S} [see Eqs. (11) and (12)] and $a(Z, W_0, r_u)$ is positive so that the two terms in Eq. (41) are of opposite sign.

TABLE IX

Predictons for as yet Unobserved First-Forbidden Beta Transitions in $A = 35$–44 Nuclei[a]

Parent	Daughter	Q_0 (keV)	$t_{1/2}$(total) (sec)	$t_{1/2}$(FFB) (sec)	BR(FFB) (%)	Possibly interesting decays: J^π	E_x (keV)	br(FFB) (%)	br(total) (%)	br(expt) (%)	$\log f_0 t$	Ref.	Remarks
^{35}Al($\frac{5}{2}^+$)	^{35}Si	14038	*b*	9.9[+0]	*b*	$\frac{7}{2}^-$	0	82.0	*b*	*b*	7.01	[18]	R1 ≃ R2
^{35}Si($\frac{7}{2}^-$)	^{35}P	10497	8.7(17)[−1]	1.2[+2]	7.40[−1]	$\frac{3}{2}^+$	2386	99.6	7.30[−1]	*c*	6.88		$B_1 = 2.26$ fm^2
^{35}P($\frac{1}{2}^+$)	^{35}S	3988	4.73(7)[+1]	1.1[+8]	4.4[−5]	$\frac{3}{2}^-$	2348	99.9	4.3[−5]	<8.0[−2]	9.76	[18]	R2 ≃ 5R1
^{36}Si(0^+)	^{36}P	7612	5.4(15)[−1]	2.2[+2]	2.5[−1]	2^-	425	87.6	2.2[−1]	*c*	7.21		$B_1 = 1.34$ fm^2
^{36}P(4^-)	^{36}S	10415	5.33(53)	3.9[+2]	1.37	2^+	3291	100.0	1.37	*c*	7.03	[47]	$B_1 = 2.29$ fm^2
^{36}K(2^+)	^{36}Ar	12805	3.42(2)[−1]	2.9[+2]	1.2[−1]	2^-	4974	13.0	1.6[−2]	<0.7	7.44		96% R0; br(FFB) = 1.5% for 3_1^-
						2^-	(6842)	67.0	8.0[−2]	*b*	6.17	*d*	98% R0
^{37}P($\frac{1}{2}^+$)	^{37}S	7896	2.31(13)	3.0[+2]	7.7[−1]	$\frac{3}{2}^-$	646	36.4	2.8[−1]	<4.0	7.59	[17]	br(FFB) ≃ 30% for $\frac{1}{21}^-$, $\frac{3}{21}^-$
^{37}K($\frac{3}{2}^+$)	^{37}Ar	6149	1.226(7)	4.8[+3]	2.5[−2]	$\frac{3}{2}^-$	2491	98.0	2.5[−2]	<1.0[−2]	5.94	*e*	98% R0; $\frac{7}{21}^-$ BR = 0.09%
^{37}Ca($\frac{3}{2}^+$)	^{37}K	11640	1.75(3)[−1]	2.7[+2]	6.5[−2]	$\frac{3}{2}^-$	2173	18.0	1.2[−2]	*b*	7.75		95 R0; $\frac{7}{21}^-$ BR = 2.9%
						$\frac{3}{2}^-$	3317	51.0	3.3[−2]	*b*	6.96	[40]	95% R0
^{38}K(3^+)	^{38}Ar	5913	4.58(1)[+2]	1.7[+6]	2.63[−4]	3^-	3810	99.2	2.6[−4]	<1.0[−2]	8.82	[40]	76% R0
^{38}Ca(0^+)	^{38}K	6742	4.47(10)[−1]	1.5[+3]	3.0[−2]	0^-	2993	92.6	2.8[−2]	*b*	5.52		
^{39}Cl($\frac{3}{2}^+$)	^{39}Ar	3438	3.34(1)[+3]	2.8[+4]	1.18[+1]	$\frac{5}{2}^-$	2092	0.03	3.6[−3]	<8.6[−3]	9.38	[36]	BR to $\frac{3}{21}^-$, $\frac{7}{21}^-$ known
^{39}Ca($\frac{3}{2}^+$)	^{39}K	6524	0.8596(14)	1.7[+4]	5.0[−3]	$\frac{3}{2}^-$	3019	97.8	5.1[−3]	<6.0[−3]	6.37	*e*	93% R0
^{40}Cl(2^-)	^{40}Ar	7513	8.10(12)[+1]	2.9[+2]	2.8[+1]	2^+	1461	27.4	7.7	<4.0	7.27	[40]	73% R0; see Tables III and IV
^{41}Ar($\frac{7}{2}^-$)	^{41}K	2492	6.58(2)[+3]	9.6[+5]	6.8[−1]	$\frac{3}{2}^+$	1560	0.02	1.4[−4]	<3.8[−3]	10.44	[45]	BR to $\frac{1}{21}^+$, $\frac{4}{21}^+$ known
^{41}Sc($\frac{7}{2}^-$)	^{41}Ca	6495	0.5963(17)	4.9[+5]	1.2[−4]	$\frac{7}{2}^+$	2883	86.0	1.0[−4]	*b*	7.21	[45]	All decays are weak
^{42}K(2^-)	^{42}Ca	3525	4.450(1)[+4]	2.6[+11]	9.93[+1]	4^+	2752	1.7[−5]	1.7[−5]	*b*	11.00	*f*	$B_1 = 0.027$ fm^2
^{42}Sc(7^+)	^{42}Ca	7041	6.16(4)[+1]	2.3[+8]	2.70[−5]	5^-	4100	72.1	1.95[−5]	*b*	10.13		$B_1 = 0.018$ fm^2
^{42}Ti(0^+)	^{42}Sc	6999	0.199(6)	1.6[+4]	5.81	0^-	(4137)	81.9	1.05[−3]	*b*	5.81	*d*	
^{43}Sc($\frac{7}{2}^-$)	^{43}Ca	2220	1.401(4)[+4]	2.1[+13]	6.7[−8]	$\frac{3}{2}^+$	990	100.0	6.7[−8]	*b*	10.92		$B_1 = 0.075$ fm^2
^{44}K(2^-)	^{44}Ca	5659	1.33(1)[+3]	2.0[+3]	6.79[+1]	2^+	1157	6.1	4.1	<3.0	8.20	[40]	13% R0

[a] Uncertain spin or parity assignments are in parentheses, as are the uncertainties in the least significant figure of the experimental values. The numbers in square brackets are powers of 10.

[b] Not known.

[c] The limit is so coarse as to be uninteresting.

[d] The level is not known; E_x is the predicted value.

[e] Deduced from results presented in Ref. [46].

[f] The BR(FFB) is the experimental value.

Typical β^+ decays are $0\hbar\omega \to 1\hbar\omega$ so that from Eqs. (11) and (12) we see that M_0^S and M_0^T have the same sign. However, $a(Z, W_0, r_u)$ usually changes sign since it is given by $r'_w\xi + \frac{1}{3}W_0$, and $r'_w\xi$—negative for β^+ decay—is usually larger than $\frac{1}{3}W_0$. Thus, we usually have destructive interference in β^+ R0 decays but not necessarily so and certainly of a lesser degree than in β^- decay since $a(Z, W_0, r_u)$ is smaller due to the destructive interference between $r'_w\xi$ and $\frac{1}{3}W_0$. In the present instance, ^{38}Ca decaying to the 2993-keV 0^- state of ^{38}K, Eq. (41) gives

$$B_1^{(0)} = [M_0^T - 2.31 \cdot M_0^S]^2 \tag{51}$$

and with our predictions for the effective matrix elements of $M_0^T = 57.7$, $M_0^S = 1.98$, the M_0^S term is 8 % of the first term. In comparison the $^{38}S(\beta^-)^{38}Cl\ 0^+ \to 0^-$ transition with $a(Z, W_0, r_u) = 4.96$ has a M_0^S term 17 % of the M_0^T term when the same effective moments are used [see Table VI]. This is one reason for the large predicted $B_1^{(0)}$ value for the $^{38}Ca\ 0^+ \to 0^-$ decay. The other is the rather simple nature of the wavefunctions. The ^{38}Ca 0^+ state is 94 % $d_{3/2}^{-2}$ while the first two 0^- states of ^{38}K are both predicted to have dominant configurations of

$$a\,|d_{3/2}^{-3}\,p_{3/2}\rangle + b\,|d_{3/2}^{-3}\,f_{7/2}\rangle + \text{remainder} \tag{52}$$

with (coincidentally) $a^2 \simeq 0.40$, $b^2 \simeq 0.28$ for both. It turns out that in this case the $\pi(d_{3/2}) \to \nu(p_{3/2})$ transition is unusually strong and dominant. It should be remarked that our predicted 0_1^- level is 1470 keV too high in excitation energy; this is the worst agreement of the WBMB interaction with experiment for an *fp* level in $A = 35$–41 nuclei.

The 0^+ ^{42}Ti branch to the as yet unobserved $^{42}Sc\ 0_1^-$ level also has a small $\log f_0 t$ value but it is predicted to be a 10^{-3} % branch and therefore considerably more difficult to observe.

In ^{39}Cl, ^{39}Ca, ^{40}Cl, and ^{44}K decays, the first-forbidden branch considered is above or not far below the present experimental limit. These also are candidates for further study.

I. Summary

1. *Introduction*

In our view the most successful and complete shell-model descriptions of nuclear observables have been the pioneer work of Cohen and Kurath [48] in the 1*p* shell and the subsequent much more extensive description of the *sd* shell by Wildenthal and collaborators as fully explored and explained in a series of articles by Brown and Wildenthal [49–52]. Since these descriptions are of a single major shell they are naturally confined to observables which are relevant to properties mainly dependent on the amplitudes of nucleons in a single major shell. Here we are concerned with nuclear states generated from occupations of more than one major

shell, specifically, cross-shell wavefunctions between the (sd) and (fp) major shells. The observables of interest are intrinsically more complicated and probe features of nuclear structure of a character different from those revealed by intra-shell observables such as M1 and E2 moments and transitions. For various reasons first-forbidden beta decay provides the simplest of these observables.

2. *Unique First-Forbidden Decays*

Once again we find it expedient to separate discussion of first-forbidden beta decay by rank. The bulk of the experimental data in the $A = 40$ region is for unique $\Delta J = 2$ decays simply because the low-lying states are dominated by $d_{3/2}^{-n} f_{7/2}^{m}$ excitations between which R0 and R1 decays are forbidden. Our present study updates the previous ones of Towner and his colleagues [2, 44] and substantiates the findings of those studies. Those findings were that the repulsive $T = 1$ particle–hole interaction causes severe inhibition of the dominant transition, for which the prototype is

$$(d_{3/2})^{A-32-n} f_{7/2}^{n} \to (d_{3/2})^{A-32-n+1} (f_{7/2})^{n-1}, \tag{53}$$

via correlations in both the initial and the final states. We are able to treat this problem more exactly in that the $d_{3/2} f_{7/2}$ model space is replaced by the full $sdpf$ space so that the transition becomes

$$(sd)^{A-16-n} (fp)^{n} \to (sd)^{A-16-n+1} (fp)^{n-1}. \tag{54}$$

This calculation then includes the correlations in the initial state added perturbatively by Towner *et al.* and fully vindicates this previous treatment. This is important because diagonalization of the ground-state correlations, i.e., expansion of Eq. (54) to include $2\hbar\omega$ terms in the final state as in

$$(sd)^{A-16-n} (fp)^{n} \to \alpha_0 [(sd)^{A-16-n+1} (fp)^{n-1}] + \alpha_2 [(sd)^{A-16-n-1} (fp)^{n+1}], \tag{55}$$

is beyond our capabilities and so we must reply on perturbative estimates of this effect. It is indeed gratifying that the observed quenching of the unique rates is in qualitative agreement with the estimates of ground-state correlations made by Towner *et al.* This means that the net effect of all other effects is predicted to be relatively small compared to the large overall factor of $(0.510)^{-2}$ left unexplained after correlations in the initial state are included.

3. $J \to J$ *First-Forbidden Decays*

As shown in Table VI, the R0 contribution dominates $\Delta J = 0$ decays in the $A \sim 40$ region just as it does at $A \sim 16$ [10]. Thus, these decays are a potential source of information on the mesonic enhancement of M_0^{T}. However, the known decays are rather weak. As shown in Table VI, the $B_1^{(0)}$ values are of order 0.1–0.2 of the single-particle estimate of ~ 90 fm for a $1d_{3/2} \to 2p_{3/2}$ transition (Table II). Thus these decays are not too informative. Nevertheless, they do seem to support

the need for mesonic enhancement found much more convincingly near $A \sim 16$. The calculations of unobserved decays summarized in Table IX do reveal one interesting transition; namely $^{38}\mathrm{Ca}(0_1^-) \rightarrow {}^{38}\mathrm{K}(0_1^-)$. This is predicted to have $\log f_0 t = 5.52$. Using the relationship [see Section E.4]

$$M_1^{(0)} = [9.15/f_0 t]^{1/2} \times 10^4 \tag{56}$$

we find $M_1^{(0)} = 53$ fm for the predicted R0 beta matrix element. This is $\sim \frac{1}{2}$ a single-particle $1d_{3/2} \rightarrow 2p_{3/2}$ transition and thus its observation would provide an interesting possibility for study of mesonic enhancement.

REFERENCES

1. E. K. WARBURTON, G. T. GARVEY, AND I. S. TOWNER, *Ann. Phys. (N.Y.)* **57** (1970), 174.
2. I. S. TOWNER, E. K. WARBURTON, AND G. T. GARVEY, *Ann. Phys. (N.Y.)* **66** (1971), 674.
3. K. KUBODERA, J. DELORME, AND M. RHO, *Phys. Rev. Lett.* **40** (1978), 755.
4. I. S. TOWNER, *Comments Nucl. Part. Phys.* **15** (1986), 145.
5. E. K. WARBURTON, *in* "Interactions and Structures in Nuclei" (R. J. Blin-Stoyle and W. D. Hamilton, Eds.), p. 81, Adam Hilger, Bristol/Philadelphia, 1988.
6. D. J. MILLENER, D. E. ALBURGER, E. K. WARBURTON, AND D. H. WILKINSON, *Phys. Rev. C* **26** (1982), 1167.
7. E. K. WARBURTON, D. E. ALBURGER, AND D. H. WILKINSON, *Phys. Rev. C* **26**, (1982), 1186.
8. E. K. WARBURTON, *Bull. Amer. Phys. Soc* **28** (1983), 726.
9. E. K. WARBURTON, D. E. ALBURGER, AND D. J. MILLENER, *Phys. Rev. C* **29** (1984), 2281.
10. D. J. MILLENER AND E. K. WARBURTON, *in* "Nuclear Shell Models" (M. Vallieres and B. H. Wildenthal, Eds.), p. 365, World-Scientific, Singapore, 1985.
11. E. K. WARBURTON, D. J. MILLENER, B. A. BROWN, AND J. A. BECKER, *Bull. Amer. Phys. Soc.* **31** (1986), 1222.
12. I. S. TOWNER AND F. C. KHANNA, *Nucl. Phys. A* **399** (1983), 334.
13. I. S. TOWNER, *Annu. Rev. Nucl. Part. Sci.* **36** (1986), 115.
14. H. BEHRENS AND W. BÜHRING, *Nucl. Phys. A* **162** (1971), 111; "Electron Radial Wave Functions and Nuclear Beta-decay," Clarendon, Oxford, 1982.
15. J. D. WALECKA, *in* "Muon Physics" (V. W. Hughes and C. S. Wu, Eds.), Vol. II, p. 113, Academic Press, New York, 1975.
16. B. A. BROWN, A. ETCHEGOYEN, W. D. M. RAE, AND N. S. GODWIN, OXBASH, 1984, unpublished.
17. E. K. WARBURTON AND J. A. BECKER, *Phys. Rev. C* **37** (1988), 754.
18. E. K. WARBURTON, D. E. ALBURGER, J. A. BECKER, B. A. BROWN, AND S. RAMAN, *Phys. Rev. C* **34** (1986), 1031.
19. H. F. SCHOPPER, "Weak Interactions and Nuclear Beta Decay," North-Holland, Amsterdam, 1966.
20. I. S. TOWNER AND J. C. HARDY, *Nucl. Phys. A* **179** (1972), 489.
21. D. H. WILKINSON, *Nucl. Phys. A* **377** (1982), 474.
22. D. M. BRINK AND G. R. SATCHLER, "Angular Momentum," Clarendon, Oxford, 1968.
23. B. A. BROWN, C. R. BRONK, AND P. E. HODGSON, *J. Phys. G* **10** (1984), 1683.
24. I. S. TOWNER AND F. C. KHANNA, *Nucl. Phys. A* **372** (1981), 331.
25. R. J. BLIN-STOYLE AND S. C. K. NAIR, *Adv. Phys.* **15** (1966), 493.
26. H. A. SMITH AND P. C. SIMMS, *Phys. Rev. C* **1** (1970), 1809.
27. P. BLUNDEN, B. CASTEL, AND H. TOKI, *Nucl. Phys. A* **440** (1985), 647.

28. S. T. HSIEH, R. B. M. MOOY, AND B. H. WILDENTHAL, *Bull. Amer. Phys. Soc.* **30** (1985), 731; S. T. HSIEH, X. JI, R. MOOY, AND B. H. WILDENTHAL, *in* "Nuclear Structure at High Spin, Excitation, and Momentum Transfer" (H. Nann, Ed.), p. 357, AIP Conf. Proc. 142, Amer. Inst. of Physics, New York, 1986.
29. G. GARVEY, "Nuclear Spectroscopy and Nuclear Interactions" (H. Ejiri and T. Fukuda, Eds.), p. 193, World-Scientific, Singapore, 1984.
30. S. NOZAWA, K. KUBODERA, AND H. OHTSUBO, *Nucl. Phys. A* **453** (1986), 645.
31. H. BEHRENS AND J. JÄNECKE, "Numerical Tables for Beta-Decay and Electron Capture," Landolt–Börnstein, New Series, Group I, Vol. 4, Springer-Verlag, Berlin, 1969.
32. W. BAMBYNEK, H. BEHRENS, M. H. CHEN, B. CRASEMANN, M. L. FITZPATRICK, K. W. D. LEDINGHAM, H. GENZ, M. MUTTERER, AND R. L. INTEMANN, *Rev. Mod. Phys.* **49** (1977), 77; Erratum, *Rev. Mod. Phys.* **49** (1977), 961.
33. D. E. ALBURGER AND E. K. WARBURTON, *Phys. Rev. C* **38**, No. 4, in press.
34. T. W. BURROWS, *Nucl. Data Sheets* **48** (1986), 569.
35. S. RAMAN AND N. B. GOVE, *Phys. Rev. C* **7** (1973), 1995.
36. G. WANG, E. K. WARBURTON, AND D. E. ALBURGER, *Phys. Rev. C* **35** (1987), 2272.
37. L. K. FIFIELD, M. A. C. HOTCHKIS, P. V. DRUMM, T. R. OPHEL, G. D. PUTT, AND D. C. WEISSER, *Nucl. Phys. A* **417** (1984), 534.
38. A. HUCK, G. KLOTZ, A. KNIPPER, C. MIEHÉ, C. RICHARD-SERRE, AND G. WALTER, *in* "4th International Conference on Nuclei far from Stability" (P. G. Hansen and O. B. Nielsen, Eds.), p. 378, CERN 81–09, Geneva, 1981.
39. E. BROWNE AND R. B. FIRESTONE, "Table of Isotopes" (V. S. Shirley, Ed.) Wiley, New York, 1986.
40. P. M. ENDT AND C. VAN DER LEUN, *Nucl. Phys. A* **310** (1978), 1.
41. A. H. WAPSTRA AND G. AUDI, *Nucl. Phys. A* **432** (1985), 1.
42. E. K. WARBURTON AND D. E. ALBURGER, submitted for publication, in Physical Review C.
43. D. FREKERS, W. HENNING, W. KUTSCHERA, K. E. REHM, R. K. SMITHER, J. L. YNTEMA, R. SANTO, B. STIEVANO, AND N. TRAUTMANN, *Phys. Rev. C* **28** (1983), 1756.
44. I. S. TOWNER, *Nucl. Phys. A* **151** (1970), 97.
45. F. JUNDT, E. ASLANIDES, A. GALLMANN, AND E. K. WARBURTON, *Phys. Rev. C* **4** (1971), 498.
46. F. M. MANN, H. S. WILSON, AND R. W. KAVANAGH, *Nucl. Phys. A* **258** (1976), 341.
47. E. K. WARBURTON AND J. A. BECKER, *Phys. Rev. C* **35** (1987), 1851.
48. S. COHEN AND D. KURATH, *Nucl. Phys.* **73** (1965), 1.
49. B. H. WILDENTHAL, *Prog. Part. Nucl. Phys.* **11** (1984), 5.
50. B. A. BROWN AND B. H. WILDENTHAL, *At. Data Nucl. Tables* **33** (1985), 347.
51. B. A. BROWN, *in* "Proceedings of the International Physics Conference, Harrogate, UK, 1986" (J. L. Durell, J. M. Irvine, and G. C. Morrison, Eds.), Vol. 2, p. 119, Institute of Physics, Bristol, 1987.
52. B. A. BROWN AND B. H. WILDENTHAL, *Nucl. Phys. A* **474** (1987), 290.